

Joint Power Optimization for Device-to-Device Communication in Cellular Networks with Interference Control

Ali Ramezani-Kebrya, *Student Member, IEEE*, Min Dong, *Senior Member, IEEE*, Ben Liang, *Senior Member, IEEE*, Gary Boudreau, *Senior Member, IEEE*, and S. Hossein Seyedmehdi

Abstract—For device-to-device (D2D) communication underlaid in a cellular network with uplink resource sharing, both cellular and D2D pairs may cause significant inter-cell interference (ICI) at a neighboring base station (BS). In this work, under optimal BS receive beamforming, we jointly optimize the power of a cellular user (CU) and a D2D pair for their sum rate maximization, while satisfying minimum SINR requirements and worst-case ICI limit in multiple neighboring cells. We solve this non-convex joint optimization problem in two steps. First, the necessary and sufficient condition for the D2D admissibility under given constraints is obtained. Next, we consider joint power control of the CU and D2D transmitters. We propose a power control algorithm to maximize the sum rate. Depending on the severity of ICI that D2D and CU may cause, we categorize the feasible solution region into five cases, each of which may further include several scenarios based on minimum SINR requirements. The proposed algorithm is optimal when ICI to a single neighboring cell is considered. For multiple neighboring cells, we provide an upper bound on the performance loss by the proposed algorithm and conditions for its optimality. We further extend our consideration to the scenario of multiple CUs and D2D pairs, and formulate the joint power control and CU-D2D matching problem. We show how our proposed solution for one CU and one D2D pair can be utilized to solve this general joint optimization problem. Simulation demonstrates the effectiveness of our power control algorithm and the nearly optimal performance of the proposed approach in the setting of multiple CUs and D2D pairs.

Index Terms—Device-to-device communication, inter-cell interference, power control, receive beamforming.

I. INTRODUCTION

The increasing popularity of mobile devices with data hungry applications has resulted in a fast growing demand for high-rate data access experiences. It is anticipated that it will be challenging for the currently deployed Long Term Evolution (LTE) and LTE-Advanced systems to satisfy such demand in the future. New technologies to further improve

the capacity and spectrum efficiency are required for future cellular system evolution. One promising solution is device-to-device (D2D) communication, in which nearby users can setup a direct communication link to transmit data to each other without going through the base station (BS), by reusing cellular spectrum resources [2]–[5]. Such resource reuse by both cellular users (CUs) and D2D pairs can offload cellular traffic and improve radio resource utilization. As a result, it is shown that D2D communication can increase the overall network spectrum efficiency [2].

For D2D communication underlaid in a cellular system to reuse spectrum resource assigned to CUs, uplink resource sharing is in general preferred for several reasons [6], [7]. Downlink spectrum reuse for D2D communication would require a D2D pair to have a new transmit chain, which is more costly than uplink spectrum reuse, where only a new receive chain is required at the D2D receiver (such as in LTE systems). In addition, uplink traffic is often lighter than downlink traffic, with uplink resources more likely being available for D2D communication. Furthermore, it is easier to manage the interference incurred at the BS [4]. When a D2D pair reuses the channel resource of a CU, they generate intra-cell interference to each other. Furthermore, both D2D and CU transmissions cause inter-cell interference (ICI) to neighboring cells. Thus, the use of D2D communication and corresponding resource allocation need to ensure satisfactory quality-of-service (QoS) for both D2D pairs and CUs, as well as to maintain a satisfactory ICI limit to neighboring cells.

For a D2D underlaid cellular network, interference management to D2Ds and CUs in the same cell has been investigated in various aspects in the literature [6]–[22]. The works in [6]–[15] focus on interference management to meet minimum QoS requirements for both D2Ds and CUs. Maximizing the sum rate of D2Ds and CUs while meeting the minimum QoS requirements through power control, resource allocation, or association techniques among users is considered in [16]–[19]. The problem of joint D2Ds and CUs association and power control to maximize the sum rate has been considered in [20], [21]. Despite the above results, the ICI due to D2D communication has not been investigated in the existing literature. For a practical system, the ICI caused by both D2Ds and CUs in a neighboring cell should be carefully controlled to not exceed a certain level. In addition, due to the challenges involved in the problem, existing power allocation schemes for interference mitigation proposed in the literature are typically

This work was funded in part by Ericsson Canada, by the Natural Sciences and Engineering Research Council (NSERC) of Canada under Collaborative Research and Development Grant CRDPJ-466072-14 and Discovery Grants.

A. Ramezani-Kebrya and B. Liang are with the Department of Electrical and Computer Engineering, University of Toronto, Toronto, Ontario M5S 3G4, Canada (e-mail: aramezani@ece.utoronto.ca; liang@ece.utoronto.ca).

M. Dong is with the Department of Electrical, Computer and Software Engineering, University of Ontario Institute of Technology, Oshawa, Ontario L1H 7K4, Canada (e-mail: min.dong@uoit.ca).

G. Boudreau and S. H. Seyedmehdi are with Ericsson Canada, Ottawa, Ontario, Canada (e-mail: gary.boudreau@ericsson.com; hossein.seyedmehdi@ericsson.com).

A preliminary version of this work was presented in [1].

heuristics whose performance gap from the optimal cannot be guaranteed.

In this work, we consider D2D communication underlaid in a cellular system for uplink resource sharing. We assume all users are equipped with a single antenna, while the BS is equipped with multiple antennas. First, we focus on one D2D pair sharing the uplink resource assigned to one CU. We aim at jointly optimizing the power control at the CU and D2D transmitters, under optimal BS receive beamforming, to maximize the sum rate of the D2D and CU while satisfying minimum SINR requirements and obeying worst-case ICI to multiple neighboring cells. The formulated joint optimization problem is non-convex. We propose a two-step approach to find a solution:

- We determine the admissibility of the D2D pair under the power, SINR, and ICI constraints, through a feasibility test. The optimal beam vector for the CU is provided, as well as the necessary and sufficient condition for the D2D admissibility.
- Assuming the D2D pair is admissible, we propose an approximate power control algorithm to maximize the sum rate. We obtain the power solution of the CU and D2D in closed form, by analyzing the feasible solution region of the problem and the characteristics of the solution in the feasible region. We show that, depending on the severity of the ICI that D2D and CU each may cause to the neighboring cell, the shape of the feasible solution region can be categorized into five cases, each of which may further include several scenarios depending on the minimum SINR requirements. With a total of sixteen unique scenarios, we derive the joint power solution in closed form for each scenario. The proposed algorithm is optimal when ICI to a single neighboring cell is considered. For ICI to multiple neighboring cells, we provide an upper bound on the performance loss by the proposed algorithm and conditions for its optimality.

Next, we extend our consideration to the scenario of multiple CUs and D2D pairs, and formulate the joint power control and CU-D2D matching problem. The joint optimization problem is a mixed integer programming problem that is difficult to solve. Instead, as a suboptimal approach, we show how our provided solution for one CU and one D2D pair can be utilized to find a solution by breaking down the joint optimization problem into a joint power optimization problem and a CU-D2D matching problem.

Simulation shows that substantial performance gain is achieved by the proposed power control algorithm over two alternative approaches for a single CU and D2D pair. Furthermore, for multiple CUs and D2D pairs, simulation shows that our proposed approach provides close to optimal performance.

A. Related Work

To limit the intra-cell interference due to resource sharing by CUs and D2Ds, different approaches have been proposed to meet minimum QoS requirements. As one of the earliest works, [8] has proposed a simple power control scheme for the D2D pair to constrain the SINR degradation of the CU,

with limited interference coordination available between D2D and CU. In [13], the interference link condition between D2D and CU is obtained through the D2D pairs' received power measurement during uplink transmission, and an interference-aware resource allocation scheme for D2D pairs has been proposed. To limit the interference at the D2D receiver, [7] has proposed an interference limited cell area, where a D2D pair and multiple CUs cannot coexist for channel reuse. For uplink resource sharing, [14] has proposed to scale the power of a D2D transmitter according to the pathloss between the D2D transmitter and the BS to satisfy the CU SINR requirement.

Without ICI consideration, the sum rate maximization of D2D and CU under their respective minimum QoS requirements has been studied in the literature. In [16], optimal time-frequency resource allocation and power control for sum rate maximization of a D2D pair and a CU has been studied, under rate limitation due to modulation and coding, and the CU's minimum QoS requirement. For a single-antenna system, optimal power allocation for sum rate maximization of a D2D pair and a CU has been obtained in [17]. In contrast, we consider a multi-antenna BS and ICI constraints when optimizing the CU and D2D powers, which is more general and technically more challenging. With only the statistics of the interfering link from a CU to a D2D pair being available at the BS, [18] have proposed a probabilistic access control for the D2D pair to maximize the expected sum rate for uplink resource sharing. A low complexity D2D-CU association scheme has been proposed in [19] to maximize the sum rate of D2D pairs and CUs under power and QoS constraints.

The gaming approach has also been considered for D2D resource sharing [22], [23]. The problem of joint association and power control for D2D pairs has been studied in [22] using a pricing-based game theoretical approach to satisfy the SINR requirements of D2D pairs and CUs. A nontransferable coalition formation game has been considered in [23] to solve the energy-efficient resource sharing problem for mobile D2D multimedia communication.

To the best of our knowledge, neither ICI to neighboring cells nor BS receive beamforming has been considered in the literature studying the joint power optimization of CU and D2D for sum rate maximization under their respective minimum SINR requirements.

B. Organization and Notations

The rest of this paper is organized as follows. In Section II, the system model is described and the sum rate maximization problem is formulated. In Section III, a closed-form expression of the optimal beam vector is derived, and the necessary and sufficient condition for admissibility of the D2D pair is obtained. The power control solution at the CU and D2D transmitter is obtained through the study of five cases of ICI conditions in Section IV. In Section V, we extend our consideration to multiple CUs and D2D pairs, and present our approach for the joint power control and CU-D2D matching problem by utilizing the previous solution. Numerical results are presented in Section VI, and conclusions are drawn in Section VII.

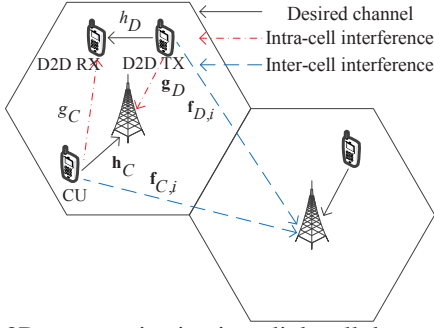


Fig. 1: D2D communication in uplink cellular communication.

Notation: We use $\|\cdot\|$ to denote the Euclidean norm of a vector. \mathbf{I} stands for an $N \times N$ identity matrix.

II. SYSTEM MODEL AND PROBLEM FORMULATION

A. System Model

We study the underlying D2D communication in a cellular system, where D2D devices reuse the spectrum resource already assigned to the CUs for their uplink communication. We assume orthogonal spectrum resource allocation among the CUs within a cell. Thus, these CUs do not interfere with each other. When a D2D pair communicates using the channel assigned to a CU, the D2D pair and the CU cause intra-cell interference to each other. We first focus on a single CU and a single D2D pair attempting to reuse the CU's channel as shown in Fig. 1. We assume that all users are equipped with a single antenna and the BS is equipped with N antennas. The BS centrally coordinates the transmission from the CU and the D2D pair. In Section V, we extend our consideration to the scenario of multiple CUs and D2D pairs.

Let P_D and P_C denote the transmit power of the D2D pair and the CU, respectively. The SINR at the D2D receiver, denoted by γ_D , is given by

$$\gamma_D = \frac{P_D |h_D|^2}{\sigma_D^2 + P_C |g_C|^2} \quad (1)$$

where $h_D \in \mathbb{C}$ is the channel between the D2D pair, $g_C \in \mathbb{C}$ is the interference channel between the CU and the D2D receiver, and σ_D^2 is the noise variance at the D2D receiver. The uplink received SINR at the BS from the CU is given by

$$\gamma_C = \frac{P_C |\mathbf{w}^H \mathbf{h}_C|^2}{\sigma^2 + P_D |\mathbf{w}^H \mathbf{g}_D|^2} \quad (2)$$

where $\mathbf{h}_C \in \mathbb{C}^{N \times 1}$ is the channel between the CU and the BS, $\mathbf{g}_D \in \mathbb{C}^{N \times 1}$ is the interference channel between the D2D transmitter and the BS, \mathbf{w} is the receive beam vector at the BS with unit norm, *i.e.*, $\|\mathbf{w}\|^2 = 1$, and σ^2 is the noise variance at the BS.¹

Both D2D and CU transmissions cause ICI in a neighboring cell. In this work, we focus on ICI for uplink transmission at neighboring BSs. However, our approach can also be applied to considering ICI in the downlink transmission scenario. Let b denote the number of neighboring cells. Let $\mathbf{f}_{C,i} \in \mathbb{C}^{N \times 1}$

and $\mathbf{f}_{D,i} \in \mathbb{C}^{N \times 1}$ denote the ICI channels from the CU and the D2D transmitter to neighboring BS i , respectively, for $i = 1, \dots, b$. Since the beam vector at neighboring BS i is typically unknown to the CU and D2D pair, we consider the worst-case ICI, denoted by $P_{\mathcal{I},i}$, given by

$$P_{\mathcal{I},i} = P_C \|\mathbf{f}_{C,i}\|^2 + P_D \|\mathbf{f}_{D,i}\|^2. \quad (3)$$

Note that $P_{\mathcal{I}}$ is an upper bound of the actual ICI, because for a neighboring BS with the beam vector $\tilde{\mathbf{w}}$, the received signal is $|\tilde{\mathbf{w}}^H \mathbf{f}| \leq \|\mathbf{f}\|$.

We assume perfect knowledge of the communication channels and intra-cell interfering channels, *i.e.*, \mathbf{h}_C , h_D , g_C , and g_D .² For the ICI channels, note that only channel power gains are needed to obtain $P_{\mathcal{I},i}$. They can be measured at neighboring BSs and shared with the BS of the desired cell through the backhaul.

B. Problem Formulation

Let P_C^{\max} and P_D^{\max} denote the maximum transmit power at the CU and D2D transmitters, respectively. Our goal is to maximize the sum rate of the D2D pair and the CU by optimizing the transmit powers $\{P_D, P_C\}$ and the receive beam vector \mathbf{w} , while satisfying the worst-case ICI and minimum SINR requirements under per-node power constraints. The problem is formulated as follows:

$$\text{P1:} \quad \max_{P_D, P_C, \mathbf{w}} \log(1 + \gamma_C) + \log(1 + \gamma_D)$$

$$\text{subject to } \gamma_C \geq \tilde{\gamma}_C, \quad (4)$$

$$\gamma_D \geq \tilde{\gamma}_D, \quad (5)$$

$$P_C \leq P_C^{\max}, P_D \leq P_D^{\max}, \quad (6)$$

$$P_{\mathcal{I},i} \leq \tilde{\mathcal{I}}, i = 1, \dots, b \quad (7)$$

where $\tilde{\gamma}_C$ and $\tilde{\gamma}_D$ are the minimum SINR requirements of the CU and D2D pair, respectively, and $\tilde{\mathcal{I}}$ is the worst-case ICI threshold in neighboring cells.

The optimization problem P1 is non-convex, due to the non-convex objective function. Solving P1 requires two steps. First, we need to determine whether the D2D pair can be admitted to reuse the CU's channel. Second, if the D2D pair can be admitted, we optimize the powers and beam vector to maximize the sum rate in P1. The first problem can be cast as a feasibility test as shown in the next section. For the second problem, we will derive the optimal power solution $\{P_D^o, P_C^o\}$ when $b = 1$. For $b > 1$, we will propose an approximate power control algorithm by applying the results obtained for $b = 1$.

III. ADMISSIBILITY OF D2D

Given the power constraints, SINR requirements, and ICI threshold, the admissibility of the D2D pair can be determined by evaluating the feasibility of the problem in P1 given by

$$\text{Find } \{P_D, P_C, \mathbf{w}\} \quad (8)$$

$$\text{subject to } (4), (5), (6), (7).$$

¹The noise term in SINR expressions, *i.e.*, σ^2 and σ_D^2 , can be treated as the receiver noise plus inter-cell interference power.

²Note that the additional signaling overhead due to D2D communication is mainly on the feedback of channels $\{h_D, g_C\}$ to the BS. These two channels are typically necessary for establishing D2D communication.

A necessary condition for P1 being feasible is that CU SINR constraint (4) under the optimal \mathbf{w} should be met for some $\{P_D, P_C\}$. For any given $\{P_C, P_D\}$, we obtain the optimal beam vector \mathbf{w}^o that maximizes γ_C . This is a receive beamforming problem given by

$$\max_{\mathbf{w}: \|\mathbf{w}\|^2=1} \frac{P_C \mathbf{w}^H \mathbf{H}_C \mathbf{w}}{\mathbf{w}^H \mathbf{\Lambda}_D \mathbf{w}} \quad (9)$$

where $\mathbf{H}_C \triangleq \mathbf{h}_C \mathbf{h}_C^H$ and $\mathbf{\Lambda}_D \triangleq \sigma^2 \mathbf{I} + P_D \mathbf{g}_D \mathbf{g}_D^H$. The maximization problem (9) is a generalized eigenvalue problem, and the optimal beam vector is given by

$$\mathbf{w}^o = \frac{\mathbf{\Lambda}_D^{-1} \mathbf{h}_C}{\|\mathbf{\Lambda}_D^{-1} \mathbf{h}_C\|}. \quad (10)$$

The SINR of the CU in (2) under the optimal \mathbf{w}^o is given by

$$\max_{\mathbf{w}} \gamma_C = P_C \mathbf{h}_C^H \mathbf{\Lambda}_D^{-1} \mathbf{h}_C \quad (11)$$

which is a function of $\{P_D, P_C\}$.

From the definition of $\mathbf{\Lambda}_D$, and applying the matrix inversion lemma [24], we derive $\mathbf{\Lambda}_D^{-1}$ as $\mathbf{\Lambda}_D^{-1} = \frac{1}{\sigma^2} \left(\mathbf{I} - \frac{P_D \mathbf{g}_D \mathbf{g}_D^H}{\sigma^2 + P_D \|\mathbf{g}_D\|^2} \right)$. Substituting the expression of $\mathbf{\Lambda}_D^{-1}$ into (11) and after some algebraic manipulation, the SINR constraint (4) under the optimal beamforming can be re-expressed as

$$\frac{P_C \|\mathbf{h}_C\|^2}{\sigma^2} \left(1 - \frac{\rho^2}{1 + \frac{\sigma^2}{P_D \|\mathbf{g}_D\|^2}} \right) \geq \tilde{\gamma}_C \quad (12)$$

where $\rho \triangleq \frac{|\mathbf{h}_C^H \mathbf{g}_D|}{\|\mathbf{h}_C\| \|\mathbf{g}_D\|}$ is the correlation coefficient of the channels \mathbf{h}_C and \mathbf{g}_D , and $|\rho| \leq 1$.

For P1 to be feasible, there should exist at least one power solution pair $\{P_D, P_C\}$ such that constraints (5)-(7) and (12) hold. For notation simplicity, in the following, we denote $x \triangleq P_D$ and $y \triangleq P_C$. We now study the SINR constraints (5) and (12) and state the following lemma.

Lemma 1: For $\gamma_D = \tilde{\gamma}_D$ and $\gamma_C = \tilde{\gamma}_C$, the power solution $\{x_{\mathcal{I}}, y_{\mathcal{I}}\}$ is unique and is given by

$$x_{\mathcal{I}} = \frac{\xi}{2(1 - K_1)}, \quad y_{\mathcal{I}} = \frac{\xi}{2(1 - K_1)\beta K_3} - \frac{\sigma_D^2}{K_3} \quad (13)$$

where $\alpha \triangleq \frac{\sigma^2 \tilde{\gamma}_C}{\|\mathbf{h}_C\|^2}$, $\beta \triangleq \frac{\tilde{\gamma}_D}{\|\mathbf{h}_D\|^2}$, $K_1 \triangleq \rho^2$, $K_2 \triangleq \frac{\sigma^2}{\|\mathbf{g}_D\|^2}$, $K_3 \triangleq |g_C|^2$, $K_4 \triangleq \beta(\alpha K_3 + \sigma_D^2(1 - K_1)) - K_2$, $K_5 \triangleq 4(1 - K_1)\beta K_2(\alpha K_3 + \sigma_D^2)$, and

$$\xi = \beta(\alpha K_3 + \sigma_D^2(1 - K_1)) - K_2 + \sqrt{K_4^2 + K_5}.$$

Proof: See Appendix A.

By Lemma 1 and combining constraints (6) and (7), the necessary and sufficient condition for the D2D pair to be admissible is given as follows.

Necessary and sufficient condition: The D2D pair is admissible if $\{x_{\mathcal{I}}, y_{\mathcal{I}}\}$ in (13) satisfies

$$0 < x_{\mathcal{I}} \leq P_D^{\max}, \quad (14)$$

$$0 < y_{\mathcal{I}} \leq P_C^{\max}, \quad (15)$$

$$c_{1,i} y_{\mathcal{I}} + c_{2,i} x_{\mathcal{I}} \leq 1, \quad i = 1, \dots, b \quad (16)$$

where $c_{1,i} \triangleq \frac{\|\mathbf{f}_{C,i}\|^2}{\mathcal{I}}$, and $c_{2,i} \triangleq \frac{\|\mathbf{f}_{D,i}\|^2}{\mathcal{I}}$.

Note that $\{x_{\mathcal{I}}, y_{\mathcal{I}}\}$ is the minimum power level required to satisfy the minimum SINR requirements. Thus, for any feasible $\{x, y\}$, we have $x \geq x_{\mathcal{I}}$ and $y \geq y_{\mathcal{I}}$. Constraints (14) and (15) ensure the maximum power at the D2D and CU are enough to meet their respective SINR requirements. Constraint (16) ensures the ICI constraints can be satisfied.

IV. POWER CONTROL FOR D2D AND CU

Assuming the D2D pair is admissible, we now solve the sum rate maximization problem P1. With the optimal \mathbf{w}^o given in (10), we need to solve P1 with respect to $\{P_D, P_C\}$. Due to the non-convex objective, finding an optimal solution is challenging. Instead, we propose the following approximation to obtain the power solution.

Note that the ICI constraints in (7) can be equivalently written as

$$c_{1,i} x + c_{2,i} y \leq 1, \quad i = 1, \dots, b. \quad (17)$$

We replace these ICI constraints with a single ICI constraint and ensure that it satisfies the ICI requirements in all neighboring cells. We denote this constraint by $c_1 y + c_2 x \leq 1$, where c_1 and c_2 are determined as follows.

Define $c_{1,\max} \triangleq \max_i c_{1,i}$, $c_{2,\max} \triangleq \max_i c_{2,i}$, $\tilde{x} \triangleq \min_i \frac{1 - c_{1,i} P_C^{\max}}{c_{2,i}}$, and $\tilde{y} \triangleq \min_i \frac{1 - c_{2,i} P_D^{\max}}{c_{1,i}}$. Note that if there exists i such that $c_{1,i} P_C^{\max} \geq 1$, then from (17), $y \leq \frac{1}{\max_i c_{1,i}}$, and we have $c_1 = c_{1,\max}$. Otherwise, if $c_{1,i} P_C^{\max} < 1$ for all i , then the intersection of $c_1 y + c_2 x = 1$ and $y = P_C^{\max}$ is given by (\tilde{x}, P_C^{\max}) . Similarly, if there exists j such that $c_{2,j} P_D^{\max} \geq 1$, then $c_2 = c_{2,\max}$. Otherwise, the intersection of $c_1 y + c_2 x = 1$ and $x = P_D^{\max}$ is given by (P_D^{\max}, \tilde{y}) . Based on this, we determine c_1 and c_2 in four possible cases:³

- 1) If $\exists i, j$, such that $c_{1,i} P_C^{\max} \geq 1$ and $c_{2,j} P_D^{\max} \geq 1$: $c_1 = c_{1,\max}$ and $c_2 = c_{2,\max}$.
- 2) If $\exists i$, such that $c_{1,i} P_C^{\max} \geq 1$, and $\forall j$, $c_{2,j} P_D^{\max} < 1$: $c_1 = c_{1,\max}$ and $c_2 = \frac{1 - c_{1,\max} \tilde{y}}{P_C^{\max}}$.
- 3) If $\forall i$, $c_{1,i} P_C^{\max} < 1$, and $\exists j$, such that $c_{2,j} P_D^{\max} \geq 1$: $c_1 = \frac{1 - c_{2,\max} \tilde{x}}{P_C^{\max}}$ and $c_2 = c_{2,\max}$.
- 4) If $\forall i, j$, $c_{1,i} P_C^{\max} < 1$ and $c_{2,j} P_D^{\max} < 1$: $c_1 = \frac{P_C^{\max} - \tilde{x}}{P_D^{\max} P_C^{\max} - \tilde{x} \tilde{y}}$ and $c_2 = \frac{P_C^{\max} - \tilde{y}}{P_D^{\max} P_C^{\max} - \tilde{x} \tilde{y}}$.

Note that when $b = 1$, the approximation becomes accurate to represent the ICI constraint. Substituting the expression of γ_C under the optimal \mathbf{w}^o at the left hand side of (12) in P1, and approximating multiple ICI constraints in (17) with a single ICI constraint, we modify P1 into the following problem

$$\text{P2: } \max_{(x,y)} \log \mathcal{R}(x, y) \quad (18)$$

$$\text{subject to } y \left(1 - \frac{K_1 x}{K_2 + x} \right) \geq \tilde{\gamma}_C, \quad (19)$$

$$\frac{\alpha x}{\sigma_D^2 + K_3 y} \geq \tilde{\gamma}_D, \quad (20)$$

$$y \leq P_C^{\max}, \quad x \leq P_D^{\max}, \quad (21)$$

$$c_1 y + c_2 x \leq 1 \quad (22)$$

³Note that other values of c_1 and c_2 may also be chosen; however, our method strives to create a new feasible region that is close to the original one, so that the loss due to approximation is small.

where

$$\mathcal{R}(x, y) \triangleq \left(1 + \frac{ax}{\sigma_D^2 + K_3y}\right) \left(1 + y\left(1 - \frac{K_1x}{K_2 + x}\right)l\right), \quad (23)$$

with $a \triangleq |h_D|^2$ and $l \triangleq \|\mathbf{h}_C\|^2/\sigma^2$.

Let \mathcal{A}_{xy} denote the feasible solution region of the problem P2. Note that by modifying P1 to P2, we shrink the original feasible region of P1 to \mathcal{A}_{xy} . This is done by replacing the feasible region boundaries formed by the intersections of the multiple ICI constraints in (17) with a single boundary described by (22). The following lemma gives the locations of the optimal power pair in \mathcal{A}_{xy} .

Lemma 2: The optimal power solution pair (x^o, y^o) is at the vertical, horizontal, or tilted boundary of \mathcal{A}_{xy} , given by $x = P_D^{\max}$, $y = P_C^{\max}$, or $c_1y + c_2x = 1$, respectively.

Proof: See Appendix B.

Note that, depending on the system parameter setting, the shape of the feasible region \mathcal{A}_{xy} varies. The boundaries of \mathcal{A}_{xy} may or may not include the tilted boundary segment $c_1y + c_2x = 1$. In the following, we consider both cases and obtain the optimal solution to P2 for each case.

If the boundaries of \mathcal{A}_{xy} do not include $c_1y + c_2x = 1$, the optimal solution satisfies (22) with strict inequality. By Lemma 2, it follows that at least one of x^o and y^o equals its maximum value (P_D^{\max} or P_C^{\max}), and the optimal (x^o, y^o) is at either the vertical or horizontal boundary line of \mathcal{A}_{xy} . In this case, the optimal power pair is given in the following proposition.

Proposition 1: If the boundaries of the feasible region \mathcal{A}_{xy} do not include $c_1y + c_2x = 1$, then the optimal power pair (x^o, y^o) for P2 is at one end point of the vertical or horizontal boundary line segment of \mathcal{A}_{xy} .

Proof: See Appendix C.

If the boundaries of \mathcal{A}_{xy} include $c_1y + c_2x = 1$, then at optimality, (x^o, y^o) is on the horizontal, vertical, or tilted boundary line of \mathcal{A}_{xy} . The following proposition provides the solution to P2 in this case.

Proposition 2: If the boundaries of the feasible region \mathcal{A}_{xy} include $c_1y + c_2x = 1$, then the optimal power pair (x^o, y^o) is given in one of the two cases: 1) An end point of the horizontal, vertical, or tilted boundary line segment of \mathcal{A}_{xy} ; or 2) an interior point of tilted boundary line segment of \mathcal{A}_{xy} , whose x -coordinate is one of the roots of the following quartic equation

$$e_4x^4 + e_3x^3 + e_2x^2 + e_1x + e_0 = 0 \quad (24)$$

where $\{e_i\}_{i=0}^4$ are given as in (D.1)–(D.5) in Appendix D. The optimal CU power is $y^o = (1 - c_2x^o)/c_1$.

Proof: See Appendix D.

Note that the roots of a quartic equation have closed-form expressions. Furthermore, we do not need to compute all the roots of (24), since not all of them are in \mathcal{A}_{xy} . In the following, we classify different scenarios leading to different types of the boundaries for \mathcal{A}_{xy} . We obtain simple inequalities to check the conditions under which each scenario applies. For each scenario, we discuss the corresponding optimal power solution (x^o, y^o) .

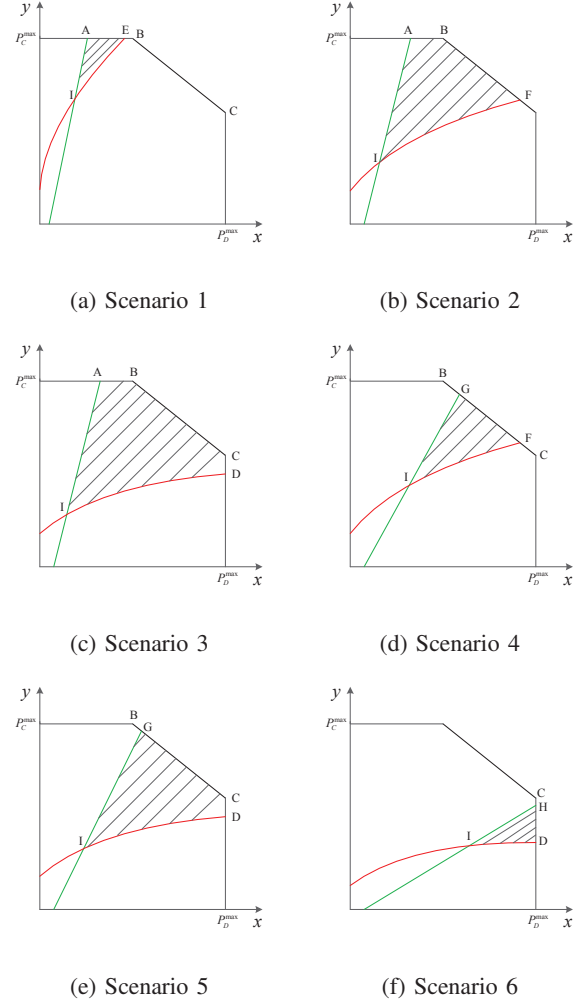


Fig. 2: Moderate ICI from CU and D2D.

A. Moderate ICI from CU and D2D

We first consider the case where the boundary line $c_1y + c_2x = 1$ intersects both the horizontal and vertical boundary lines. This means that $c_1P_C^{\max} + c_2P_D^{\max} \geq 1$, and the x -intercept and y -intercept of $c_1y + c_2x = 1$ are greater than P_D^{\max} and P_C^{\max} , respectively. These result in the following conditions

$$\frac{1 - c_2P_D^{\max}}{c_1} \leq P_C^{\max} \leq \frac{1}{c_1}, \quad (25)$$

$$\frac{1 - c_1P_C^{\max}}{c_2} \leq P_D^{\max} \leq \frac{1}{c_2}. \quad (26)$$

Note that given the definitions of c_1 and c_2 , conditions (25) and (26) mean that the ICI caused by the CU or D2D transmitter alone, at each maximum power, is less than the ICI threshold, while combined the ICI caused by both of them is greater than the ICI threshold. In other words, both the CU and the D2D transmitter cause relatively moderate ICI to the neighboring cell.

In this case, depending on SINR requirements (19) and (20), there are several different shapes of the feasible region \mathcal{A}_{xy} , as shown in Figs. 2a–2f, where \mathcal{A}_{xy} is the shaded area. The curve

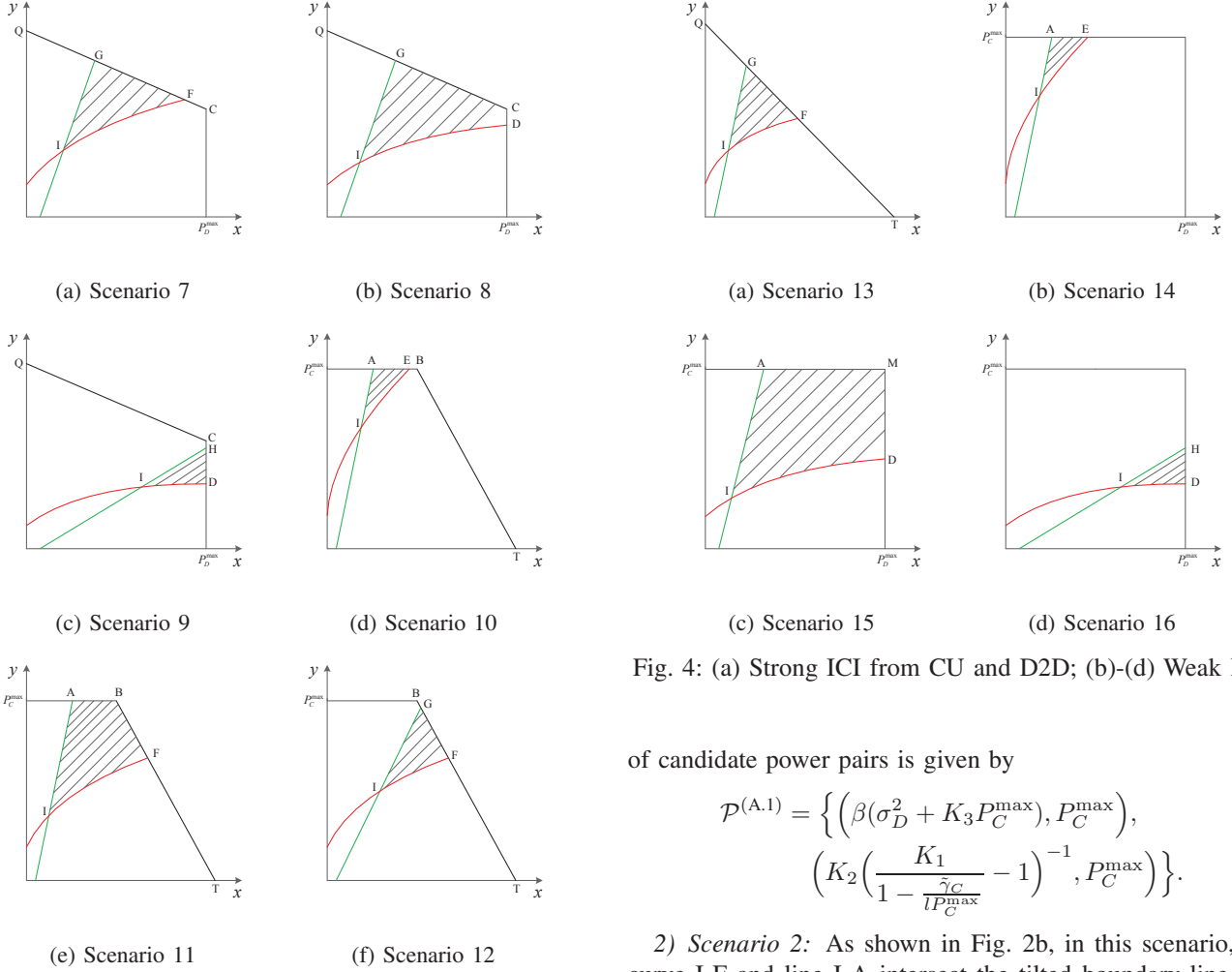


Fig. 3: (a)-(c) Strong ICI from CU and moderate ICI from D2D; (d)-(f) Moderate ICI from CU and strong ICI from D2D.

and line passing through point I correspond to constraints (19) and (20) with equality. The feasible region \mathcal{A}_{xy} 's in Figs. 2a–2f correspond to six scenarios, depending on whether the line and curve passing through point I intersect the vertical, horizontal, or tilted boundary. In the following, we derive the optimal power control solution in each of these six scenarios.

1) *Scenario 1*: The feasible solution region \mathcal{A}_{xy} is depicted in Fig. 2a as the shaded area. Points A, B, C, E, and I are the intersections of two lines (or a line and curve). Both curve I-E and line I-A intersect with the horizontal boundary line $y = P_C^{\max}$. In this scenario, we have $x_E \leq x_B$. It occurs under the following condition:

$$K_2 \left(\frac{K_1}{1 - \frac{\gamma_C}{lP_C^{\max}}} - 1 \right)^{-1} \leq \frac{1 - c_1 P_C^{\max}}{c_2}. \quad (27)$$

By Lemma 2 and Proposition 1, the optimal power pair (x^o, y^o) can be one of points A and E. Therefore, the set

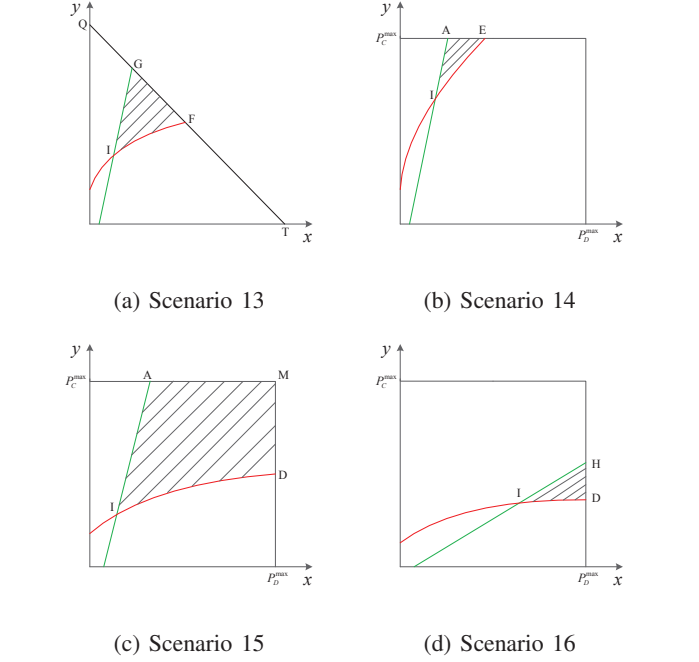


Fig. 4: (a) Strong ICI from CU and D2D; (b)-(d) Weak ICI.

of candidate power pairs is given by

$$\mathcal{P}^{(A,1)} = \left\{ \left(\beta(\sigma_D^2 + K_3 P_C^{\max}), P_C^{\max} \right), \left(K_2 \left(\frac{K_1}{1 - \frac{\gamma_C}{lP_C^{\max}}} - 1 \right)^{-1}, P_C^{\max} \right) \right\}. \quad (28)$$

2) *Scenario 2*: As shown in Fig. 2b, in this scenario, the curve I-F and line I-A intersect the tilted boundary line and horizontal boundary line, respectively. Note that x_F is the x -coordinate of point F, which is the intersection of the curve I-F and the tilted boundary line B-F. We can find x_F by setting constraints (19) and (22) with equality. This results in a quadratic equation given by

$$c_2(1 - K_1)x^2 - \theta x + K_2(\alpha c_1 - 1) = 0 \quad (29)$$

where $\theta \triangleq 1 - K_1 - c_2 K_2 - \alpha c_1$. The uniqueness of the feasible solution of (29) is stated in the following lemma.

Lemma 3: For \mathcal{A}_{xy} as shown in Fig. 2b, the feasible solution of the quadratic equation (29) is unique and is given by

$$x_F = \frac{\theta + \sqrt{\theta^2 - 4c_2(1 - K_1)K_2(\alpha c_1 - 1)}}{2c_2(1 - K_1)}. \quad (30)$$

Proof: See Appendix E.

Note that in Scenario 2, we have $x_A \leq x_B \leq x_F \leq P_D^{\max}$. The conditions for this scenario to happen are as follows:

$$\beta(\sigma_D^2 + K_3 P_C^{\max}) \leq \frac{1 - c_1 P_C^{\max}}{c_2}, \quad (31)$$

$$\frac{1 - c_1 P_C^{\max}}{c_2} \leq x_F \leq P_D^{\max}. \quad (32)$$

By Proposition 2, the candidate pairs for (x^o, y^o) are points A, B, F, and any interior point of line B-F. For the last case

to happen, x^o should be within the range $\frac{1-c_1P_C^{\max}}{c_2} < x^o < x_F$, which means the roots of (24) should satisfy this range constraint. Let \mathcal{S}_2 be the set of roots that meet the above range constraint. The corresponding set of points on the interior of line B-F is given by $\mathcal{A}_2 \triangleq \{(x, (1-c_2x)/c_1) : x \in \mathcal{S}_2\}$.

Now, we have the set of candidate pairs for (x^o, y^o) as

$$\mathcal{P}^{(A.2)} = \left\{ \left(\beta(\sigma_D^2 + K_3P_C^{\max}), P_C^{\max} \right), \left(x_F, (1-c_2x_F)/c_1 \right), \left((1-c_1P_C^{\max})/c_2, P_C^{\max} \right), \mathcal{A}_2 \right\} \quad (33)$$

where the first three pairs are the coordinates for points A, F, and B, respectively.

3) *Scenario 3*: As illustrated in Fig. 2c, in this scenario, the curve I-D and line I-A intersect the horizontal and vertical boundary lines, respectively. The entire tilted boundary B-C is in the feasible region. In this scenario, we have $x_A \leq x_B$ and $y_D \leq y_C$. The conditions for this scenario to occur are given by

$$\alpha \left(1 - \frac{K_1}{1 + K_2/P_D^{\max}} \right)^{-1} \leq \frac{1 - c_2P_D^{\max}}{c_1}, \quad (34)$$

and (31).

By Proposition 2, (x^o, y^o) could be either points A, B, C, D, or if (x^o, y^o) lies on the interior of line B-C, x^o should be within the range $x_B < x^o < x_C$, i.e., $\frac{1-c_1P_C^{\max}}{c_2} < x^o < P_D^{\max}$.

Let \mathcal{S}_3 denote the set of roots (24) satisfying the above range constraint. By Proposition 2, the set of candidate pairs on the interior of line B-C is given by $\mathcal{A}_3 \triangleq \{(x^o, (1-c_2x^o)/c_1) : x \in \mathcal{S}_3\}$.

Thus, in Scenario 3, the set of candidate pairs is given by

$$\mathcal{P}^{(A.3)} = \left\{ \left(\beta(\sigma_D^2 + K_3P_C^{\max}), P_C^{\max} \right), \left((1-c_1P_C^{\max})/c_2, P_C^{\max} \right), \left(P_D^{\max}, (1-c_2P_D^{\max})/c_1 \right), \left(P_D^{\max}, \alpha \left(1 - \frac{K_1}{1 + K_2/P_D^{\max}} \right)^{-1} \right), \mathcal{A}_3 \right\} \quad (35)$$

where the first four pairs are the coordinates of points A, B, C, and D, respectively.

4) *Scenario 4*: As shown in Fig. 2d, in this scenario, both curve I-F and line I-G intersect the tilted boundary line B-C. The condition for this scenario to happen is as follows:

$$\frac{1 - c_1P_C^{\max}}{c_2} \leq x_G \leq x_F \leq P_D^{\max} \quad (36)$$

where x_G can be obtained by setting constraints (20) and (22) with equality, given by

$$x_G = \frac{\sigma_D^2\beta + \beta K_3/c_1}{1 + \beta K_3 c_2/c_1}. \quad (37)$$

By Proposition 2, to find the optimal power pair, we need to consider points G and F. The set of candidate power pairs on the interior of line G-F is given by $\mathcal{A}_4 \triangleq \{(x^o, (1-c_2x^o)/c_1) : x \in \mathcal{S}_4\}$ where \mathcal{S}_4 denotes the set of roots (24) which meet $x_G < x^o < x_F$.

Thus, the set of candidate pairs is given as follows:

$$\mathcal{P}^{(A.4)} = \left\{ \left(x_G, (1-c_2x_G)/c_1 \right), \left(x_F, (1-c_2x_F)/c_1 \right), \mathcal{A}_4 \right\}. \quad (38)$$

TABLE I: Moderate ICI from CU and D2D (under conditions (25) and (26))

Condition	Set of candidates for the optimal powers
(27)	$\mathcal{P}^o = \mathcal{P}^{(A.1)}$ in (28)
(31) and (32)	$\mathcal{P}^o = \mathcal{P}^{(A.2)}$ in (33)
(31) and (34)	$\mathcal{P}^o = \mathcal{P}^{(A.3)}$ in (35)
(36)	$\mathcal{P}^o = \mathcal{P}^{(A.4)}$ in (38)
(34) and (39)	$\mathcal{P}^o = \mathcal{P}^{(A.5)}$ in (40)
(41)	$\mathcal{P}^o = \mathcal{P}^{(A.6)}$ in (42)

5) *Scenario 5*: As shown in Fig. 2e, in this scenario, line I-G intersects tilted boundary line G-C, while curve I-D intersects the vertical boundary line $x = P_D^{\max}$. In this scenario, we have $x_B \leq x_G \leq P_D^{\max}$ and $y_D \leq y_C$. The conditions under which this scenario happens are given by

$$\frac{1 - c_1P_C^{\max}}{c_2} \leq x_G \leq P_D^{\max}, \quad (39)$$

and (34).

Based on Proposition 2, (x^o, y^o) could be either points G, C, D, or if (x^o, y^o) is on the interior of line G-C, x^o should be within the range $x_G < x^o < P_D^{\max}$.

Let \mathcal{S}_5 denote the set of roots of (24) within the above range of x^o . The set of candidate points on the interior of line G-C is $\mathcal{A}_5 \triangleq \{(x^o, (1-c_2x^o)/c_1) : x \in \mathcal{S}_5\}$.

Hence, the set of candidate pairs for (x^o, y^o) in this scenario is given by

$$\mathcal{P}^{(A.5)} = \left\{ \left(x_G, \frac{1-c_2x_G}{c_1} \right), \left(P_D^{\max}, (1-c_2P_D^{\max})/c_1 \right), \left(P_D^{\max}, \alpha \left(1 - \frac{K_1}{1 + K_2/P_D^{\max}} \right)^{-1} \right), \mathcal{A}_5 \right\}. \quad (40)$$

6) *Scenario 6*: As depicted in Fig. 2f, this scenario happens when both curve I-D and line I-H intersect the vertical boundary line $x = P_D^{\max}$. In this scenario, we have $y_H \leq y_C$. The condition for this scenario to happen is given by

$$\frac{P_D^{\max} - \beta\sigma_D^2}{\beta K_3} \leq \frac{1 - c_2P_D^{\max}}{c_1}. \quad (41)$$

In this scenario, the boundaries of \mathcal{A}_{xy} do not include the tilted boundary line. By Proposition 1, it is sufficient to consider only points H and D to find the optimal power solution. The set of candidates for the optimal powers is thus given by

$$\mathcal{P}^{(A.6)} = \left\{ \left(P_D^{\max}, \alpha \left(1 - \frac{K_1}{1 + K_2/P_D^{\max}} \right)^{-1} \right), \left(P_D^{\max}, \frac{P_D^{\max} - \beta\sigma_D^2}{\beta K_3} \right) \right\}. \quad (42)$$

We summarize in Table I the candidate solution sets for the above six scenarios for the case where conditions (25) and (26) hold.

B. Strong ICI from CU and Moderate ICI from D2D

Consider the case in which the tilted line $c_1y + c_2x = 1$ only intersects the vertical line $x = P_D^{\max}$, but does not intersect the horizontal line $y = P_C^{\max}$. This means that the x -intercept and

y -intercept of $c_1y + c_2x = 1$ are greater than P_D^{\max} and less than P_C^{\max} , respectively. The resulting conditions are given by

$$\frac{1}{c_1} \leq P_C^{\max}, \quad (43)$$

and (26).

Note that the condition (43) means the ICI caused by the CU under its maximum power is greater than the ICI threshold. Along with (26), these conditions correspond to the case where the ICI caused by the CU is strong, while the ICI caused by the D2D transmitter is moderate.

In this case, by SINR requirements (19) and (20), the necessary and sufficient condition to set up D2D communication is given by (14) and (16). The feasible region \mathcal{A}_{xy} can have three different shapes as shown in Figs. 3a–3c, depending on whether the line and curve passing through point I intersect the vertical or tilted boundary line. Accordingly, we derive the optimal power control solution in these three scenarios as follows.

1) *Scenario 7*: As shown in Fig. 3a, in this scenario, both curve I-F and line I-G intersect the tilted boundary line. The condition under which this scenario happens is given by

$$0 \leq x_G \leq x_F \leq P_D^{\max} \quad (44)$$

where x_F and x_G are given in (30) and (37), respectively.

Let $\mathcal{P}^{(B.1)}$ denote the set of candidate pairs in this scenario. Note that the feasible region \mathcal{A}_{xy} has the same shape as that in Scenario 4 in Fig. 2d. Thus, these two scenarios have the same set of candidate pairs, *i.e.*, $\mathcal{P}^{(B.1)} = \mathcal{P}^{(A.4)}$.

2) *Scenario 8*: As depicted in Fig. 3b, in this scenario, line I-G and curve I-D intersect the tilted boundary line G-C and vertical boundary line, respectively. This scenario occurs when $x_G \leq x_C$ and $y_D \leq y_C$, which results in the following conditions:

$$0 \leq x_G \leq P_D^{\max}, \quad (45)$$

and (34).

From Fig. 3b, we see that the shape of \mathcal{A}_{xy} is the same as that of Scenario 5 in Fig. 2e. Thus, these two scenarios have the same set of candidate pairs. Let $\mathcal{P}^{(B.2)}$ denote the set of candidate power pairs in Scenario 8. We have $\mathcal{P}^{(B.2)} = \mathcal{P}^{(A.5)}$.

3) *Scenario 9*: As illustrated in Fig. 3c, this scenario happens when both curve I-D and line I-H intersect the vertical boundary line. By similar discussion as the above, the condition for this scenario to happen is the same as that in Scenario 6 in Fig. 2f, which is given by (41). As a result, the set of candidate pairs, denoted by $\mathcal{P}^{(B.3)}$, is the same as that in Scenario 6, *i.e.*, $\mathcal{P}^{(B.3)} = \mathcal{P}^{(A.6)}$.

The candidate solution sets for these three scenarios for the case with conditions (26) and (43) are summarized in Table II.

C. Moderate ICI from CU and Strong ICI from D2D

Now consider the case in which line $c_1y + c_2x = 1$ only intersects the horizontal line $y = P_C^{\max}$, but does not intersect the vertical line $x = P_D^{\max}$. Similar to the discussion in Section IV-B, this means that the x -intercept and y -intercept

TABLE II: Strong ICI from CU and Moderate ICI from D2D (under conditions (26) and (43))

Condition	Set of candidates for the optimal powers
(44)	$\mathcal{P}^o = \mathcal{P}^{(B.1)} = \mathcal{P}^{(A.4)}$
(34) and (45)	$\mathcal{P}^o = \mathcal{P}^{(B.2)} = \mathcal{P}^{(A.5)}$
(41)	$\mathcal{P}^o = \mathcal{P}^{(B.3)} = \mathcal{P}^{(A.6)}$

of $c_1y + c_2x = 1$ are greater than P_C^{\max} and less than P_D^{\max} , respectively, which are equivalent to the following conditions:

$$\frac{1}{c_2} \leq P_D^{\max}, \quad (46)$$

and (25).

These conditions correspond to the case where the ICI caused by the CU is moderate, while the ICI caused by the D2D transmitter is strong. Similar to the previous cases, depending on the SINR requirements (19) and (20), the feasible region of \mathcal{A}_{xy} can have three different shapes as shown in Figs. 3d–3f. The optimal power pair for each of these three scenarios are discussed below.

1) *Scenario 10*: The feasible region is shown in Fig. 3d. In this scenario, both curve I-E and line I-A intersect the horizontal boundary line. The shape of the feasible region \mathcal{A}_{xy} is the same as that of Scenario 1, with the condition to occur given by (27). Thus, the set of candidate pairs, denoted by $\mathcal{P}^{(C.1)}$, is given by $\mathcal{P}^{(C.1)} = \mathcal{P}^{(A.1)}$.

2) *Scenario 11*: As shown in Fig. 3e, this scenario happens when curve I-F and line I-A intersect the tilted boundary line B-F and horizontal boundary line, respectively. In this scenario, we have $x_A \leq x_B \leq x_F \leq x_T$, which results in the following conditions:

$$\frac{1 - c_1 P_C^{\max}}{c_2} \leq x_F \leq \frac{1}{c_1}, \quad (47)$$

and (31).

Similarly, the shape of \mathcal{A}_{xy} is the same as that of Scenario 2 in Fig. 2b. As a result, the set of candidate pairs, denoted by $\mathcal{P}^{(C.1)}$, is given by $\mathcal{P}^{(C.1)} = \mathcal{P}^{(A.2)}$.

3) *Scenario 12*: As depicted in Fig. 3f, in this scenario, both curve I-F and line I-G intersect the tilted boundary line. With a similar approach, we can derive the condition for this scenario to happen as follows:

$$\frac{1 - c_1 P_C^{\max}}{c_2} \leq x_G \leq x_F \leq \frac{1}{c_2}. \quad (48)$$

Again, \mathcal{A}_{xy} in this scenario has the same shape as that in Scenario 4, and thus, the set of candidate pairs, denoted by $\mathcal{P}^{(C.3)}$, is given by $\mathcal{P}^{(C.3)} = \mathcal{P}^{(A.4)}$.

The candidate solution sets for these three scenarios for the case with conditions (25) and (46) are summarized in Table III.

D. Strong ICI from CU and D2D

When the tilted line $c_1y + c_2x = 1$ does not intersect either the vertical or horizontal line, we have the feasible region \mathcal{A}_{xy} as shown in Fig. 4a. In this case the x -intercept and y -intercept of $c_1y + c_2x = 1$ are less than P_D^{\max} and P_C^{\max} ,

TABLE III: Moderate ICI from CU and Strong ICI from D2D (under conditions (25) and (46))

Condition	Set of candidates for the optimal powers
(27)	$\mathcal{P}^o = \mathcal{P}^{(C.1)} = \mathcal{P}^{(A.1)}$
(31) and (47)	$\mathcal{P}^o = \mathcal{P}^{(C.2)} = \mathcal{P}^{(A.2)}$
(48)	$\mathcal{P}^o = \mathcal{P}^{(C.3)} = \mathcal{P}^{(A.4)}$

respectively, which are equivalent to conditions (43) and (46). In this scenario, the necessary and sufficient condition to have an admissible D2D pair is reduced to (16).

Denote this case by *Scenario 13*. In this scenario, we have

$$0 \leq x_G \leq x_F \leq \frac{1}{c_2}. \quad (49)$$

Since \mathcal{A}_{xy} in both this scenario and Scenario 4 have the same shape, the set of candidate pairs, denoted by $\mathcal{P}^{(D.1)}$, is given by $\mathcal{P}^{(D.1)} = \mathcal{P}^{(A.4)}$.

E. Weak ICI

In all above cases, the line $c_1y + c_2x = 1$ intersects at least one of the horizontal and vertical boundary lines (i.e., $y = P_D^{\max}$ and $x = P_C^{\max}$).

Now we consider the case where there is no intersection between $c_1y + c_2x = 1$ and either of the horizontal and vertical boundary lines. This case happens when

$$c_1P_C^{\max} + c_2P_D^{\max} < 1. \quad (50)$$

Note that condition (50) occurs when both the CU and the D2D transmitter cause weak ICI to the neighboring cell, e.g., they both are located near the center of the cell.

Shown in Figs. 4b–4d, there are three possible shapes for the feasible region \mathcal{A}_{xy} in this case, depending the SINR requirements (19) and (20). The optimal power pairs for these three scenarios are discussed as follows.

1) *Scenario 14*: As shown in Fig. 4b, this scenario happens when curve I-E and line I-A intersect the horizontal boundary line. The condition for this scenario to happen is $x_E \leq P_D^{\max}$, i.e.,

$$K_2 \left(\frac{K_1}{1 - \frac{\tilde{\gamma}_C}{P_C^{\max}}} - 1 \right)^{-1} \leq P_D^{\max}. \quad (51)$$

Since the shape of \mathcal{A}_{xy} is the same as that in Scenario 1, the set of candidates for the optimal powers, denoted by $\mathcal{P}^{(E.1)}$, is given by $\mathcal{P}^{(E.1)} = \mathcal{P}^{(A.1)}$.

2) *Scenario 15*: As illustrated in Fig. 4c, in this scenario, line I-A and curve I-D intersect the horizontal and vertical boundary lines, respectively. In this scenario, we have $x_A \leq P_D^{\max}$ and $y_D \leq P_C^{\max}$. Solving for x_A and y_D , we have the following conditions:

$$\beta(\sigma_D^2 + K_3P_C^{\max}) \leq P_D^{\max}, \quad (52)$$

$$\alpha \left(1 - \frac{K_1}{1 + K_2/P_D^{\max}} \right)^{-1} \leq P_C^{\max}. \quad (53)$$

TABLE IV: Weak ICI (under condition (50))

Condition	Set of candidates for the optimal powers
(51)	$\mathcal{P}^o = \mathcal{P}^{(E.1)} = \mathcal{P}^{(A.1)}$
(52) and (53)	$\mathcal{P}^o = \mathcal{P}^{(E.2)}$ in (54)
(55)	$\mathcal{P}^o = \mathcal{P}^{(E.3)} = \mathcal{P}^{(A.6)}$

Algorithm 1 Approximate power control algorithm

Input: $\alpha, \beta, a, l, K_1, K_2, K_3, \{c_{1,i}, c_{2,i}\}_{i=1}^b, \tilde{\gamma}_C, \tilde{\gamma}_D, P_C^{\max}, P_D^{\max}$
Output: P_D^o, P_C^o , and \mathbf{w}^o

- 1: Check the feasibility condition (14)–(16).
- 2: Determine $c_1, c_2, a_1, a_2, b_1, b_2, x_F$, and x_G .
- 3: **if** (25) and (26) hold **then**
- 4: Compute candidate solution set in Table I.
- 5: **else if** (26) and (43) hold **then**
- 6: Compute candidate solution set in Table II.
- 7: **else if** (25) and (46) hold **then**
- 8: Compute candidate solution set in Table III.
- 9: **else if** (43) and (46) hold **then**
- 10: Compute candidate solution set $\mathcal{P}^o = \mathcal{P}^{(D.1)}$ in Section IV-D.
- 11: **else if** (50) holds **then**
- 12: Compute candidate solution set in Table IV.
- 13: **end if**
- 14: Enumerate among candidate solution set \mathcal{P}^o to find the optimum solution.
- 15: Obtain the optimum beam vector (10) using P_C^o and P_D^o .

By Proposition 1, (x^o, y^o) could be at either of points A, D, or M, and the set of candidate pairs is given by

$$\mathcal{P}^{(E.2)} = \left\{ \left(\beta(\sigma_D^2 + K_3P_C^{\max}), P_C^{\max} \right), \left(P_D^{\max}, P_C^{\max} \right), \left(P_D^{\max}, \alpha \left(1 - \frac{K_1}{1 + K_2/P_D^{\max}} \right)^{-1} \right) \right\}. \quad (54)$$

3) *Scenario 16*: The feasible region is shown in Fig. 4d. This scenario happens when both line I-H and curve I-D intersect the vertical boundary line. The condition for this scenario to occur is $y_H \leq P_C^{\max}$, i.e.,

$$\frac{P_D^{\max} - \beta\sigma_D^2}{\beta K_3} \leq P_C^{\max}. \quad (55)$$

Since the shape of \mathcal{A}_{xy} is the same as that in Scenario 6, the set of candidate pairs, denoted by $\mathcal{P}^{(E.3)}$, is given by $\mathcal{P}^{(E.3)} = \mathcal{P}^{(A.6)}$.

The candidate solution sets for these three scenarios for the case with condition (50) are represented in Table IV.

Finally, we summarize the steps to solve the optimization problem P1 in Algorithm 1. We note that the optimal solution in any scenario can be obtained in closed form.

F. Performance Bound Analysis

Note that Algorithm 1 is very efficient in obtaining the power solution pair $\{P_D^o, P_C^o\}$, as the candidate pairs are all given in closed-form. However, it only provides the optimal solution for $b = 1$. For $b > 1$, since \mathcal{A}_{xy} is a subset of the original feasible region of P1, Algorithm 1 is suboptimal. In the following, we provide an upper bound on the performance loss of the proposed algorithm and provide the conditions for its optimality.

Let \mathcal{A}_{xy}^o denote the original feasible region of P1, and we have $\mathcal{A}_{xy} \subseteq \mathcal{A}_{xy}^o$. An example for $b = 2$ is shown in

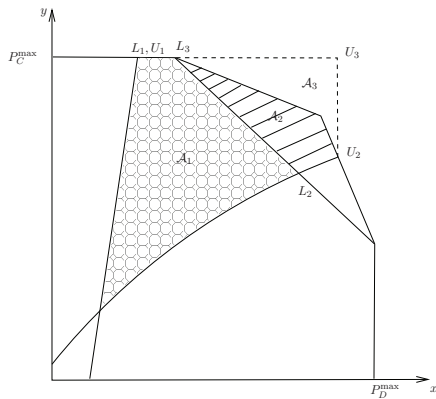


Fig. 5: Approximating the true feasible region.

Fig. 5, where \mathcal{A}_{xy} and \mathcal{A}_{xy}^o are given by \mathcal{A}_1 and $\mathcal{A}_1 \cup \mathcal{A}_2$, respectively. Let points U_1 and U_2 denote the intersections of the boundary of \mathcal{A}_{xy}^o with the line and curve corresponding to minimum SINR requirements (20) and (19), respectively. It follows that $x_{U_1} \leq x_{U_2}$ and $y_{U_2} \leq y_{U_1}$. Similarly, let points L_1 and L_2 denote the intersections of the boundary of \mathcal{A}_{xy} with the same line and curve, and we have $x_{L_1} \leq x_{L_2}$ and $y_{L_2} \leq y_{L_1}$. We denote the set of all *corner* points of \mathcal{A}_{xy} by \mathcal{L} , e.g., $\mathcal{L} = \{L_1, L_2, L_3\}$ in Fig. 5. Note that $|\mathcal{L}| \leq 4$. We define a new point $U_3 = (\max(x_{U_1}, x_{U_2}), \max(y_{U_1}, y_{U_2}))$ (as shown in Fig. 5 for $b = 2$). For simplicity, we use R_Z to denote $\log \mathcal{R}(x_Z, y_Z)$ in (18) for point Z in \mathcal{A}_{xy} . Also, let R^{A_1} and R^{opt} denote the sum rate achieved by Algorithm 1 and the maximum sum rate under an optimal solution of P1, respectively. We have the following results on the performance of Algorithm 1.

Proposition 3: For $b = 1$, $R^{\text{opt}} = R^{A_1}$. For $b > 1$, the performance loss of Algorithm 1 is bounded by

$$R^{\text{opt}} - R^{A_1} \leq \max\{R_{U_1}, R_{U_2}, R_{U_3}\} - \max_{l \in \mathcal{L}}\{R_l\}. \quad (56)$$

Furthermore, $R^{\text{opt}} = R^{A_1}$ if one of the following conditions holds:

- 1) ICI constraints in (17) results in a single tilted boundary line for \mathcal{A}_{xy}^o .
- 2) $x_{L_1} = x_{L_2}$ or equivalently $x_{U_1} = x_{U_2}$.
- 3) $y_{L_1} = y_{L_2}$ or equivalently $y_{U_1} = y_{U_2}$.

Proof: See Appendix F.

Note that in Proposition 3, Condition 1) means $\mathcal{A}_{xy} = \mathcal{A}_{xy}^o$. For Conditions 2) or 3), the line and curve associated with (20) and (19) both intersect either the vertical or horizontal boundary of \mathcal{A}_{xy}^o .

V. EXTENSION TO MULTIPLE CUs AND D2D PAIRS

So far, we have provided a power control solution for one CU and one D2D pair. We now extend our consideration to the scenario of multiple CUs and D2D pairs. Consider a multichannel communication system (e.g., OFDMA) with N_C orthogonal subchannels in each cell. We assume a fully loaded network with N_C CUs, and there are N_D D2D pairs with $N_D \leq N_C$. Without loss of generality, we assume CU j uses subchannel j for $j \in \mathcal{C} \triangleq \{1, \dots, N_C\}$. Each

D2D pair reuses at most one subchannel, and the subchannel of each CU can be reused by at most one D2D pair. Define indicator $x_{k,j} \in \{0, 1\}$ such that $x_{k,j} = 1$ if D2D pair k reuses CU j 's subchannel and $x_{k,j} = 0$ otherwise. Let $\mathbf{P} \triangleq [P_{D,1}, \dots, P_{D,N_D}, P_{C,1}, \dots, P_{C,N_C}]^T$, $\mathbf{x} \triangleq [x_{1,1}, \dots, x_{1,N_C}, \dots, x_{N_D,N_C}]^T$, and $\mathbf{w} \triangleq [\mathbf{w}_1^T, \dots, \mathbf{w}_{N_C}^T]^T$.

The objective is to maximize the overall sum rate of all D2D pairs and CUs by optimizing the transmit power vector \mathbf{P} , the indicator vector \mathbf{x} , and the receive beam vector \mathbf{w} , while satisfying the worst-case ICI and minimum SINR requirements under per-node power constraints. The formulated problem is given by⁴

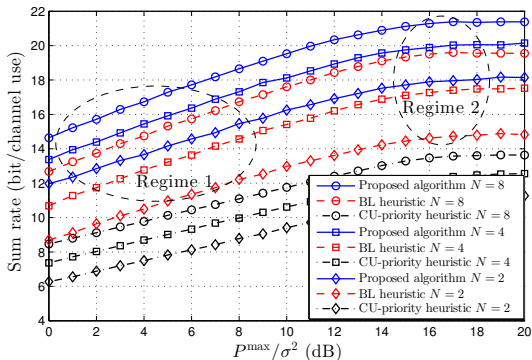
$$\begin{aligned} \text{P3: } \quad & \max_{\mathbf{P}, \mathbf{w}, \mathbf{x}} \sum_{k \in \mathcal{D}} \sum_{j \in \mathcal{C}} \log(1 + \gamma_{C,j}) + x_{k,j} \log(1 + \gamma_{D,k}) \\ \text{subject to } & \frac{P_{C,j} |\mathbf{w}_j^H \mathbf{h}_{C,j}|^2}{\sigma^2 + x_{k,j} P_{D,k} |\mathbf{w}_j^H \mathbf{g}_{D,k}|^2} \geq \tilde{\gamma}_C, \quad \forall j \in \mathcal{C} \\ & \frac{P_{D,k} |h_{D,k}|^2}{\sigma_{D,k}^2 + x_{k,j} P_{C,j} |g_{j,k}|^2} \geq \tilde{\gamma}_D, \quad \forall k \in \mathcal{D} \\ & P_{C,j} \leq P_C^{\max}, \quad P_{D,k} \leq P_D^{\max}, \quad \forall j \in \mathcal{C}, k \in \mathcal{D} \\ & P_{\mathcal{L},i,j} \leq \tilde{I}, \quad \forall j \in \mathcal{C}, i = 1, \dots, b \\ & \sum_{k \in \mathcal{D}} x_{k,j} \leq 1, \quad \sum_{j \in \mathcal{C}} x_{k,j} \leq 1, \quad \forall j \in \mathcal{C}, k \in \mathcal{D} \\ & x_{k,j} \in \{0, 1\}, \quad \forall j \in \mathcal{C}, k \in \mathcal{D} \end{aligned}$$

where \mathcal{D} denotes the set of admissible D2D pairs. D2D pair k is admissible if it can reuse at least one subchannel from \mathcal{C} .

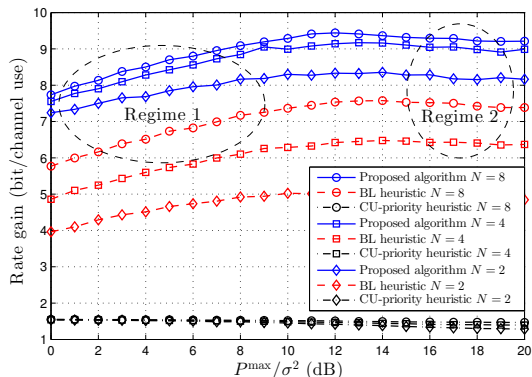
Note that problem P3 is a mixed integer programming problem and is challenging to solve. Instead, we consider a suboptimal approach by utilizing our proposed Algorithm 1 as follows:

- 1) Determine the admissibility of any D2D pair k to reuse CU j 's subchannel, for $k = 1, \dots, N_D, j = 1, \dots, N_C$.
- 2) For all k and j , if D2D pair k is admissible to use CU j 's subchannel, we jointly optimize their transmit powers to maximize their sum rate, which is given by problem P1 with the solution provided by Algorithm 1.
- 3) We solve the CU-D2D matching problem to optimally assign each admissible D2D pair to a CU. In particular, we define a bipartite graph between CUs and D2D pairs. Each edge between a D2D pair and a CU indicates that the pairing of the D2D pair and the CU is feasible. The weight of the edge is given by the sum rate or rate gain of the D2D pair and the CU, under the approximate power control solution provided by Algorithm 1. This CU-D2D matching problem is an assignment problem, whose optimal solution can be achieved by using the well-known Hungarian algorithm [26].

⁴For overall system optimization to maximize the sum rate, one would need to jointly optimize the subchannel assignment for multiple CUs and D2D pairs, and power allocation for them. This problem is known in the literature to be NP-hard [25]. In addition, re-allocating resources to all CUs and D2D pairs whenever a new D2D pair join or leave the system will increase the signaling overhead significantly. Instead, our problem formulation aims for practical design, where the addition of a D2D pair does not disturb the existing subchannel assignments for CUs.



(a) Sum rate



(b) Rate gain

Fig. 6: The sum rate and rate gain versus P^{\max}/σ^2 ($d_D/d_0 = 0.2$).

Remark 1: Note that the suboptimality of the above approach lies only in the approximation of multiple ICI constraints by a single ICI constraint. It follows that this approach is optimal for P3 if one of the conditions in Proposition 3 is satisfied.

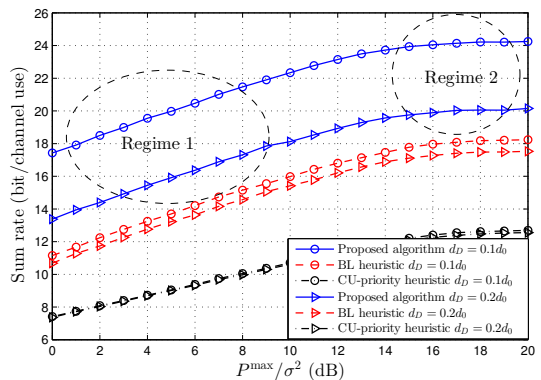
We can further reduce the complexity of the CU-D2D assignment problem in Step 3 above by proposing two suboptimal CU-D2D matching schemes. Instead of the reward (rate or gain), we define the cost on an edge between D2D pair k and CU j in the bipartite graph as follows:

- The intra-cell interference channel gain between CU j and D2D receiver k , i.e., $|g_{j,k}|$ (termed *Suboptimal CU-D2D matching A*).
- The weight of D2D transmit power in the ICI constraint (22), i.e., c_2 for D2D pair k on subchannel j (termed *Suboptimal CU-D2D matching B*).

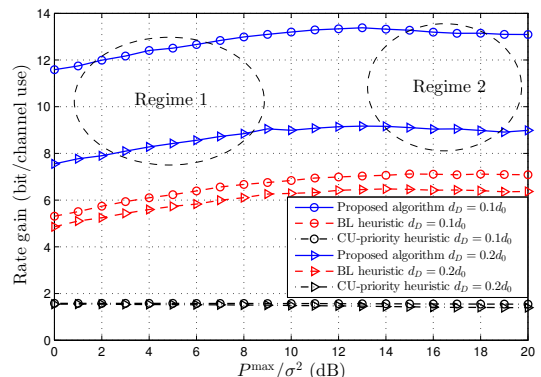
We will show through simulation that our proposed approach provides performance very close to that of the jointly optimal solution for P3.

VI. NUMERICAL RESULTS

In our simulation, we consider that the cell of interest contains one CU and one D2D pair. Assume that the BS is located at coordinates $(0,0)$, and that the CU, the D2D transmitter, and the D2D receiver are located at $(0,0.5d_0)$, $(0,-0.75d_0 - d_D/2)$, and $(0,-0.75d_0 + d_D/2)$, respectively.



(a) Sum rate

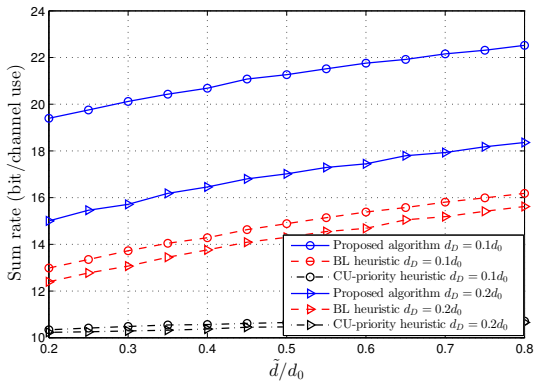


(b) Rate gain

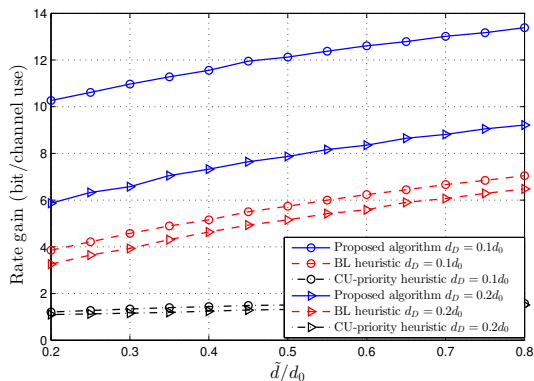
Fig. 7: The sum rate and rate gain versus P^{\max}/σ^2 ($N = 4$).

Unless otherwise mentioned, we consider one neighboring cell with its BS located at $(2d_0, 0)$. Let d_C , d_{gC} , and d_{gD} denote the distances between the CU and the BS, the CU and the D2D receiver, and the D2D transmitter and the BS, respectively, and let d_{fC} and d_{fD} denote the distance between the CU and the neighboring BS, and the D2D transmitter and the neighboring BS, respectively. We set $d_C = 0.5d_0$, $d_{gC} = 1.25d_0 - d_D/2$, $d_{gD} = 0.75d_0 + d_D/2$, $d_{fC} = 2.0616d_0$, and $d_{fD} = \sqrt{2^2 + (0.75 + 0.5d_D/d_0)^2}d_0$. For all the links, we assume the path loss exponent is set to 4. The channel coefficients are assumed to be Gaussian with zero-mean and variance $(d/d_0)^{-4}$. We set $\sigma^2 = \sigma_D^2 = 1$, $\tilde{\gamma}_C = \tilde{\gamma}_D = 3$ dB, $P_C^{\max} = P_D^{\max} = P^{\max}$, and $\tilde{I} = NI_0$ where I_0 is the ICI threshold reference, such that \tilde{I} is a function of the number of antennas at the BS. We set $I_0/\sigma^2 = 3$ dB. We use 5000 channel realizations to evaluate the average performance.

We evaluate the rate gain obtained by adding D2D communication. It is the difference of the maximum sum rate of P1 provided by Algorithm 1 and that when there is no D2D pair in the cell. Furthermore, for performance comparison, we consider two baseline algorithms: 1) *boost-and-limit (BL) heuristic*, where the unique power solution $(x_{\mathcal{I}}, y_{\mathcal{I}})$ in (13) is boosted proportionally with a common factor ζ_{\max} such that either the maximum power constraint (21) or the ICI limit (22) is met with equality, i.e., further boosting the powers would violate at least one constraint. This BL algorithm is



(a) Sum rate



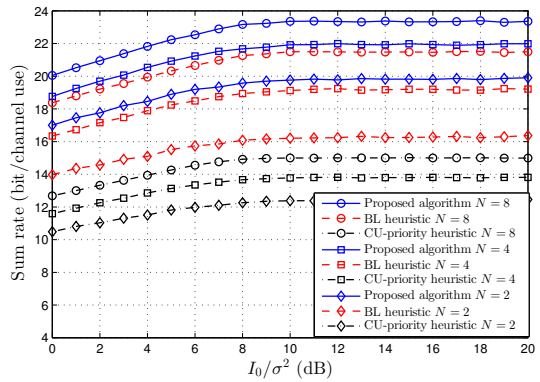
(b) Rate gain

Fig. 8: The sum rate and rate gain versus \tilde{d}/d_0 ($N = 4$, $P^{\max}/\sigma^2 = 10$ dB).

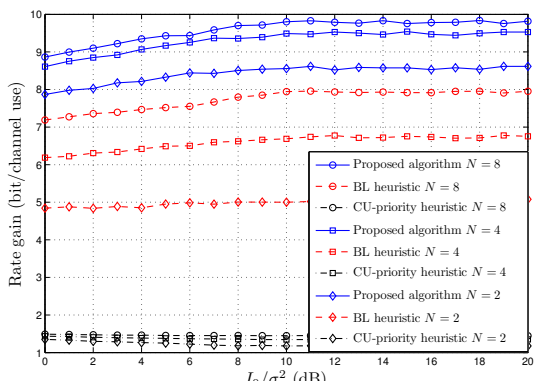
also promising in a practical point of view. Note that the scheduling BS can easily compute $(x_{\mathcal{I}}, y_{\mathcal{I}})$ and then boost the power of the CU and D2D pair until either the maximum power is achieved or a neighboring cell alerts regarding the ICI level. This can be achieved by simple binary feedback through the backhaul. Hence, there is no need for any ICI channel exchange among the cells, which reduces signaling overhead substantially. 2) *CU-priority heuristic*, aiming at maximizing SINR γ_C of the CU. It selects the maximum feasible CU power with the minimum feasible D2D power, satisfying constraints (19)–(22). Note that in this CU-priority heuristic, we prioritize the CU in terms of choosing a specific end point of the feasible region.

A. Single Neighboring Cell

We first evaluate how the performance changes with the maximum transmit power. The sum rate and rate gain versus the normalized maximum power, P^{\max}/σ^2 , under Algorithm 1, the BL heuristic, and the CU-priority heuristic, are shown in Figs. 6a and 6b, respectively, for $N = 2, 4, 8$. In Fig. 6a, for the increment of the sum rate and rate gain over P^{\max}/σ^2 under Algorithm 1, we observe two regimes: i) Regime 1, where the sum rate is an increasing function of P^{\max} . In this regime, the ICI is relatively weak, which is similar to the case in Section IV-E. In this case, as shown in Scenarios 14–16, the



(a) Sum rate

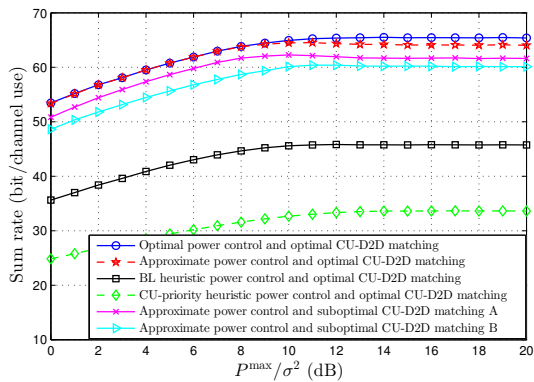


(b) Rate gain

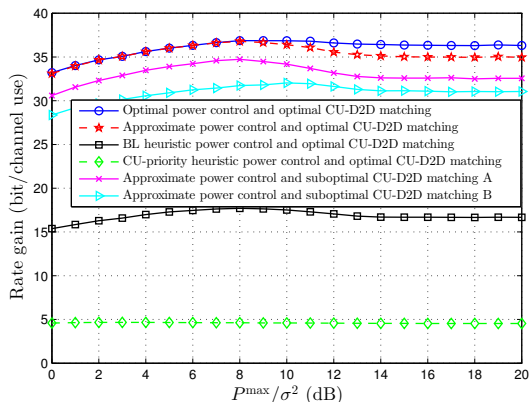
Fig. 9: The sum rate and rate gain versus I_0/σ^2 ($d_D/d_0 = 0.2$, $P^{\max}/\sigma^2 = 20$ dB).

feasible region is not affected by the ICI constraint, and the candidates for the optimal power pair in Table IV are directly functions of P^{\max} . As a result, the sum rate increases linearly with P^{\max} in this regime. ii) Regime 2, where the sum rate converges. In this regime, the ICI is relatively strong, which is similar to the case in Section IV-D. In this case, as shown in Scenario 13, the feasible region is not changed by P^{\max} , and the candidates for the optimal power pair are functions of \tilde{I} . Hence, the sum rate is controlled by the fixed ICI threshold. We observe in Fig. 6b that the rate gain is increasing in Regime 1 and decreasing in Regime 2. To see why this happens, notice that, the ICI in the D2D mode is caused by both the CU and the D2D transmitter, while in the non-D2D mode, it is caused by the CU only. Hence, in non-D2D mode, the CU can use a higher power for transmission, and the corresponding rate gain by the D2D mode is reduced. Furthermore, comparing these three algorithms, we see that the optimal solution by the proposed algorithm provides significant sum rate improvement over the BL and CU-priority heuristics in both regimes for all values of N . Note that the BL heuristic outperforms the CU-priority heuristic.

In order to study the effect of the D2D distance on the performance, the sum rate and rate gain versus P^{\max}/σ^2 for $d_D/d_0 = 0.1$ and 0.2 are shown in Figs. 7a and 7b, respectively. We set $N = 4$. Note that for the proposed



(a) Sum rate



(b) Rate gain

Fig. 10: The sum rate and rate gain versus P^{\max}/σ^2 ($N = 4$, $d_D/d_0 = 0.1$, $b = 6$).

algorithm, the sum rate and rate gain improve significantly as d_D/d_0 decreases. However, the performance of the CU-priority heuristic is not sensitive to d_D/d_0 . This is due to the objective of the sum rate of both the D2D and CU in Algorithm 1, resulting in significant rate improvement when the D2D channel is very strong, *i.e.*, the D2D distance is small.

Let \tilde{d} denote the D2D-BS distance, which is defined as the distance between the middle point of the D2D pair and the BS. The D2D transmitter and receiver are placed at $(0, -\tilde{d} - d_D/2)$ and $(0, -\tilde{d} + d_D/2)$, respectively. Then we have $d_{gC} = 0.5d_0 + \tilde{d} - d_D/2$, $d_{gD} = \tilde{d} + d_D/2$ and $d_{fD} = \sqrt{2^2 + (d_{gD}/d_0)^2}d_0$. Figs. 8a and 8b show the sum rate and rate gain versus \tilde{d}/d_0 , respectively. We set $N = 4$, $P^{\max}/\sigma^2 = 10$ dB, and $d_D/d_0 = 0.1$ and 0.2 . Increasing \tilde{d} increases the distance between the CU and the D2D pair, resulting in reduced intra-cell interference at the BS and at the D2D receiver. Furthermore, the distance between the D2D transmitter and the neighboring BS increases, which leads to ICI reduction. As expected, both the sum rate and rate gain improve as \tilde{d}/d_0 increases. Furthermore, we observe from Fig. 8b that the gap of the rate gain between the optimal solution by Algorithm 1 and the CU-priority heuristic is significant; and it increases as the D2D-BS distance increases.

We now study the effect of the ICI threshold reference I_0 on the performance. The sum rate and the rate gain versus

I_0/σ^2 are shown in Figs. 9a and 9b, respectively, for $d_D/d_0 = 0.2$ and $P^{\max}/\sigma^2 = 20$ dB. We observe that both the sum rate and rate gain improve when I_0 increases. For small I_0 values, the sum rate is an increasing function of I_0/σ^2 since the ICI is relatively strong (the case in Section IV-D), and the candidates for the optimal power pair are functions of I_0/σ^2 . As I_0 increases, the ICI constraint becomes inactive as the case in Section IV-E and the sum rate converges due to the fixed P^{\max} .

B. Multiple Neighboring Cells and Multiple Users

We now consider multiple neighboring cells and study the performance of Algorithm 1. Besides multiple neighboring cells, we further consider multiple CUs and D2D pairs in the cell of interest as discussed in Section V. We set the number of neighboring cells as $b = 6$. We consider 3 CUs and 3 D2D pairs that are randomly dropped in the cell of interest. We compare the following schemes: 1) optimal power control and optimal CU-D2D matching, where the optimal power control is obtained by exhaustive search; 2) proposed approach in Section V, *i.e.*, the approximate power control (Algorithm 1) and optimal CU-D2D matching; 3) BL heuristic power control and optimal CU-D2D matching; 4) CU-priority heuristic power control and optimal CU-D2D matching; 5) approximate power control and suboptimal CU-D2D matching A given in Section V; 6) approximate power control and suboptimal CU-D2D matching B given in Section V.

In Figs. 10a and 10b, the sum rate and rate gain versus P^{\max}/σ^2 under different power control methods and matching schemes are shown. We set $N = 4$ and $d_D/d_0 = 0.1$. We observe that the performance of our proposed approach is close to that of the optimal power control with optimal CU-D2D matching. In particular, in the region where the sum rate is an increasing function of P^{\max} , the performance by both power control schemes overlap. This demonstrates the merit of our proposed approximate power control algorithm to provide a simple closed-form solution. In addition, it can be seen that the approximate power control algorithm with any of the three CU-D2D matching schemes outperforms the BL and CU-priority heuristics with optimal CU-D2D matching. Furthermore, for the approximate power control algorithm, the gap between optimal CU-D2D matching and suboptimal CU-D2D matching A is small. This is because when CU-D2D matching A is used to define the bipartite graph, the intra-cell interference a CU causes to the matched D2D receiver is small. This results in a high D2D rate.

Note that unlike the optimal CU-D2D matching solution, where the optimal powers for pairing each D2D pair and a CU are needed to determine the best matching, for the suboptimal CU-D2D matching A scheme, only the channel power of the intra-cell interference channel needs to be known at the BS. As a result, the computational complexity of suboptimum CU-D2D matching A is drastically reduced.

VII. CONCLUSION

In this paper, we have studied power control to maximize the sum rate of a CU and a D2D pair, subject to minimum

SINR requirements, power constraints, and worst-case ICI constraints to neighboring cells. With optimal BS receive beamforming for uplink transmission, we have proposed an efficient approximate power control algorithm to obtain the powers of the CU and D2D transmitters in closed form. Depending on the ICI conditions from the CU and the D2D pair, we have divided the problem into five cases, each including several different scenarios due to minimum SINR requirements. The proposed algorithm is optimal when the ICI to a single neighboring cell is considered. For multiple neighboring cells, we have given a performance bound on our proposed algorithm, and further provided conditions for which our approximation becomes optimal.

We have further considered the general scenario of multiple CUs and D2D pairs, and have shown how our previously proposed solution can be utilized to find a solution to the joint power control and CU-D2D matching problem. Simulation demonstrates that substantial performance gain can be achieved by our proposed power control algorithm over two alternative approaches. It also shows our proposed approach provides close to optimal performance for the scenario of multiple CUs and D2D pairs, despite its low complexity. Finally, we note that studying the sum rate maximization problem in a scenario with imperfect CSI is an interesting topic for future work.

APPENDIX A PROOF OF LEMMA 1

Proof: Considering (12) with equality, we rewrite it as

$$y = \eta(x) \triangleq \alpha \left(1 - \frac{K_1}{1 + K_2/x}\right)^{-1} \quad (\text{A.1})$$

where $\alpha \triangleq \frac{\sigma^2 \tilde{\gamma}_C}{\|\mathbf{h}_C\|^2}$, $K_1 \triangleq \rho^2$, and $K_2 \triangleq \frac{\sigma^2}{\|\mathbf{g}_D\|^2}$. Taking the first and second derivatives, we have

$$\begin{aligned} \frac{d\eta(x)}{dx} &= \frac{\alpha K_1 K_2}{(x + K_2)^2} \left(1 - \frac{K_1}{1 + K_2/x}\right)^{-2} > 0, \\ \frac{d^2\eta(x)}{dx^2} &= \frac{2\alpha K_1 K_2 (K_1 - 1)}{(x + K_2)^3} \left(1 - \frac{K_1}{1 + K_2/x}\right)^{-3} \leq 0, \end{aligned}$$

since $K_1 \leq 1$ and $K_2 > 0$, *i.e.*, $\eta(x)$ is a concave strictly increasing function. Note that constraint (5) is characterized by a line on the power plane, *i.e.*, $\frac{x}{\sigma_D^2 + K_3 y} = \beta$.

Solving the intersection of this line and the curve (A.1), we obtain (13). ■

APPENDIX B PROOF OF LEMMA 2

Proof: Given any power pair (x, y) in the interior of \mathcal{A}_{xy} , there exists $\zeta > 1$, such that $(\zeta x, \zeta y) \in \mathcal{A}_{xy}$. In the following, we show that $\mathcal{R}(\zeta x, \zeta y) > \mathcal{R}(x, y)$. Substituting $(\zeta x, \zeta y)$ into (23), we have

$$\mathcal{R}(\zeta x, \zeta y) = \left(1 + \frac{ax}{\sigma_D^2/\zeta + K_3 y}\right) (1 + \Phi(\zeta)) \quad (\text{B.1})$$

where $\Phi(\zeta) \triangleq \zeta y \left(1 - \frac{K_1 x}{K_2/\zeta + x}\right) l$.

It is straightforward to show that $1 + \frac{ax}{\sigma_D^2/\zeta + K_3 y} > 1 + \frac{ax}{\sigma_D^2 + K_3 y}$ for $\zeta > 1$. In order to complete the proof, it is

sufficient to show that $\Phi(\zeta)$ is an increasing function of ζ for a given (x, y) . Taking the first derivative, we have

$$\frac{d\Phi(\zeta)}{d\zeta} = ly \frac{xK_2(1 - K_1) + \varphi}{\zeta(x + K_2/\zeta)^2} > 0 \quad (\text{B.2})$$

where $\varphi \triangleq \zeta x^2(1 - K_1) + K_2/\zeta(K_2/\zeta + x(1 - K_1))$ since $K_1 \leq 1$ and $\varphi > 0$. Therefore, we have $\mathcal{R}(\zeta x, \zeta y) > \mathcal{R}(x, y)$, *i.e.*, the optimal solution pair (x^o, y^o) is not in the interior of \mathcal{A}_{xy} . ■

APPENDIX C PROOF OF PROPOSITION 1

Proof: Substituting $y = P_C^{\max}$ and $x = P_D^{\max}$ into (23), we define $h(x) \triangleq \mathcal{R}(x, P_C^{\max})$ and $g(y) \triangleq \mathcal{R}(P_D^{\max}, y)$. To show that the maximum of $g(y)$ for $\tilde{a} \leq y \leq \tilde{b}$ is obtained when y^o is at either \tilde{a} or \tilde{b} , it is sufficient to show that $g(y)$ is a strictly monotonic function, or $g(y)$ is a strictly convex function. In the following, we show that $g(y)$ is such a function. In both cases, since P2 is a maximization problem, y^o is an end point of the domain determined by \mathcal{A}_{xy} . A similar proof is also provided for $h(x)$.

The function $g(y)$ can be written as $g(y) = (1 + \frac{\alpha_1}{\alpha_2 + y})(1 + \alpha_3 y)$ where $\alpha_1 \triangleq aP_D^{\max}/K_3$, $\alpha_2 \triangleq \sigma_D^2/K_3$, and $\alpha_3 \triangleq l\left(1 - \frac{K_1 P_D^{\max}}{K_2 + P_D^{\max}}\right)$.

Taking the first derivative of $g(y)$, we have

$$\frac{dg(y)}{dy} = \frac{\alpha_3 y^2 + 2\alpha_2 \alpha_3 y + \mu}{(\alpha_2 + y)^2} \quad (\text{C.1})$$

where $\mu \triangleq \alpha_3 \alpha_2^2 + \alpha_1(\alpha_2 \alpha_3 - 1)$. Since $\alpha_2 > 0$, $\alpha_3 > 0$, and $y \geq 0$, either $\frac{dg(y)}{dy} > 0$, *i.e.*, $g(y)$ is a strictly increasing function or $\frac{dg(y)}{dy} = 0$ may have a valid solution only if $\mu < 0$. Supposing $\mu < 0$ and taking the second derivative, we have $\frac{d^2g(y)}{dy^2} = \frac{2\alpha_1(1 - \alpha_2 \alpha_3)}{(\alpha_2 + y)^3} > 0$, since $\mu < 0$ implies $\alpha_1(1 - \alpha_2 \alpha_3) > 0$. In other words, $g(y)$ is a convex function.

Similarly, $h(x)$ can be written as $h(x) = (1 + \beta_1 x) \left(1 + \beta_2 \left(1 - \frac{K_1}{K_2/x + 1}\right)\right)$ where $\beta_1 \triangleq \frac{a}{\sigma_D^2 + K_3 P_C^{\max}}$ and $\beta_2 \triangleq lP_C^{\max}$. Taking the first derivative of $h(x)$, we have $\frac{dh(x)}{dx} = \frac{\hat{h}(x) + \omega}{(x + K_2)^2}$ where $\hat{h}(x) \triangleq \beta_1(1 + \beta_2(1 - K_1))x^2 + 2\beta_1 K_2(1 + \beta_2(1 - K_1))x$ and $\omega \triangleq \beta_1 K_2^2 + \beta_1 \beta_2 K_2^2 - \beta_2 K_1 K_2$. Since $K_1 \leq 1$, $K_2 > 0$, $\beta_1 > 0$, $\beta_2 > 0$, and $x \geq 0$, either $h(x)$ is a strictly increasing function or $\frac{dh(x)}{dx} = 0$ may have a valid solution only if $\omega < 0$. Supposing $\omega < 0$ and taking the second derivative of $h(x)$, we have $\frac{d^2h(x)}{dx^2} = \frac{2\beta_1 K_2(1 + \beta_2(1 - K_1))K_2 - 2\omega}{(x + K_2)^3} > 0$, *i.e.*, $h(x)$ is a convex function. ■

APPENDIX D PROOF OF PROPOSITION 2

Proof: By Proposition 1, if $x^o = P_D^{\max}$ or $y^o = P_C^{\max}$, then (x^o, y^o) is an end point of the vertical or horizontal boundary line segment of \mathcal{A}_{xy} , respectively. If ICI constraint

(22) is active at optimality, the optimal power is the solution of the following optimization problem:

$$\max_{(x,y)} \left(1 + \frac{ax}{\sigma_D^2 + K_3y}\right) \left(1 + y\left(1 - \frac{K_1x}{K_2+x}\right)l\right)$$

subject to $c_1y + c_2x = 1$.

Substituting $y = (1 - c_2x)/c_1$ into the objective function above, we have $\max_x \tilde{\mathcal{R}}(x)$, where $\tilde{\mathcal{R}}(x) \triangleq \left(1 + \frac{ax}{a_1 - K_4x}\right) \left(1 + (b_1 - b_2x)\left(1 - \frac{K_1x}{K_2+x}\right)\right)$. Since $\tilde{\mathcal{R}}(x)$ is continuous and has a first-order derivative, the optimum x^o is either the x -coordinate of an end point of the tilted line segment of \mathcal{A}_{xy} or obtained by solving $d\tilde{\mathcal{R}}(x)/dx = 0$, which results in the quartic equation $e_4x^4 + e_3x^3 + e_2x^2 + e_1x + e_0 = 0$ where

$$e_0 \triangleq aa_1K_2^2(b_1 + 1) - a_1^2b_1K_1K_2 - a_1^2b_2K_2^2 \quad (\text{D.1})$$

$$e_1 \triangleq -2aa_1b_2K_2^2 + aa_1K_2(b_1 + 1) - 2aa_1K_1K_2b_1 + aa_1b_1K_2 + 2a_1^2b_2K_2(K_1 - 1) + 2a_1a_2b_2K_2^2 + aa_1K_2 + 2a_1a_2b_1K_1K_2 \quad (\text{D.2})$$

$$e_2 \triangleq aa_1b_2K_2(3K_1 - 4) + aa_1(1 + b_1(1 - K_1)) + a_2b_1K_1K_2(a - a_2) - 4a_1a_2b_2K_2(K_1 - 1) + a_2b_2K_2^2(a - a_2) - a_1^2b_2(1 - K_1) \quad (\text{D.3})$$

$$e_3 \triangleq -2aa_1b_2(1 - K_1) + 2a_1a_2b_2(1 - K_1) - 2a_2b_2K_2(K_1 - 1)(a - a_2) \quad (\text{D.4})$$

$$e_4 \triangleq a_2(a - a_2)b_2(1 - K_1), \quad (\text{D.5})$$

with $a_1 \triangleq \sigma_D^2 + K_3/c_1$, $a_2 \triangleq K_3c_2/c_1$, $b_1 \triangleq l/c_1$, and $b_2 \triangleq lc_2/c_1$. ■

APPENDIX E PROOF OF LEMMA 3

Proof: We show that the alternative solution of the quadratic equation is not feasible, *i.e.*,

$$\hat{x}_F \triangleq \frac{\theta - \sqrt{\theta^2 - 4c_2(1 - K_1)K_2(\alpha c_1 - 1)}}{2c_2(1 - K_1)} < 0. \quad (\text{E.1})$$

In order to reject \hat{x}_F , it is sufficient to show that $\alpha c_1 < 1$. Substituting P_C^{\max} into (12) and considering $\rho^2 \leq 1$, we have

$$\frac{P_C^{\max} \|\mathbf{h}_C\|^2}{\sigma^2} > \tilde{\gamma}_C. \quad (\text{E.2})$$

Rearranging the inequality (E.2), we have $\alpha c_1 < c_1 P_C^{\max} < 1$, where the first and second inequality hold due to the definition of α and condition of moderate ICI from CU (25), respectively. ■

APPENDIX F PROOF OF PROPOSITION 3

Proof: Defining $R_L \triangleq \max_{l \in \mathcal{L}} \{R_l\}$, we have

$$R^{A_1} \geq R_L. \quad (\text{F.1})$$

A new feasible region $\bar{\mathcal{A}}_{xy} = \mathcal{A}_{xy}^o \cup \mathcal{A}_3$ is formed by replacing the corner of \mathcal{A}_{xy}^o with a rectangular one including U_3 . Since $\mathcal{A}_{xy}^o \subseteq \bar{\mathcal{A}}_{xy}$, we have

$$R^{\text{opt}} \leq R_U = \max\{R_{U_1}, R_{U_2}, R_{U_3}\} \quad (\text{F.2})$$

where the right-hand side of (F.2) is the optimal sum rate within $\bar{\mathcal{A}}_{xy}$ by Proposition 1. Combining (F.1) and (F.2), we have the upper bound on the sum-rate loss of Algorithm 1 given by (56).

Based on Condition 1), we have $\mathcal{A}_{xy} = \mathcal{A}_{xy}^o$, and thus the solution of Algorithm 1 is optimal. For Conditions 2), it means the line and curve associated with (20) and (19), respectively, both intersect the vertical boundary of \mathcal{A}_{xy}^o , *i.e.*, $L_1 = U_1$ and $L_2 = U_2$. In this case, by definition of U_3 , we have $U_3 = U_1$. By (F.1) and (F.2), we have $\max\{R_{U_1}, R_{U_2}\} \leq R^{A_1} \leq R^{\text{opt}} \leq \max\{R_{U_1}, R_{U_2}\}$. Thus, $R^{A_1} = R^{\text{opt}}$. For Condition 3), the line and curve both intersect the horizontal boundary of \mathcal{A}_{xy}^o with $L_1 = U_1$ and $L_2 = U_2$. Following a similar argument, we have $U_3 = U_2$, and $R^{A_1} = R^{\text{opt}}$. ■

REFERENCES

- [1] A. Ramezani-Kebrya, M. Dong, B. Liang, G. Boudreau, and S. H. Seyedmehdi, "Optimal power allocation in device-to-device communication with SIMO uplink beamforming," in *Proc. IEEE SPAWC*, Stockholm, Sweden, June 2015, pp. 425–429.
- [2] K. Doppler, M. Rinne, C. Wijting, C. Ribeiro, and K. Hugl, "Device-to-device communication as an underlay to LTE-Advanced networks," *IEEE Commun. Mag.*, vol. 47, pp. 42–49, Dec. 2009.
- [3] G. Fodor, E. Dahlman, G. Mildh, S. Parkvall, N. Reider, G. Miklós, and Z. Turányi, "Design aspects of network assisted device-to-device communications," *IEEE Commun. Mag.*, vol. 50, pp. 170–177, Mar. 2012.
- [4] X. Lin, J. G. Andrews, A. Ghosh, and R. Ratasuk, "An overview of 3GPP device-to-device proximity services," *IEEE Commun. Mag.*, vol. 52, pp. 40–48, Apr. 2014.
- [5] M. N. Tehrani, M. Uysal, and H. Yanikomeroglu, "Device-to-device communication in 5G cellular networks: challenges, solutions, and future directions," *IEEE Commun. Mag.*, vol. 52, pp. 86–92, May 2014.
- [6] H. Min, W. Seo, J. Lee, S. Park, and D. Hong, "Reliability improvement using receive mode selection in the device-to-device uplink period underlying cellular networks," *IEEE Trans. Wireless Commun.*, vol. 10, pp. 413–418, Feb. 2011.
- [7] H. Min, J. Lee, S. Park, and D. Hong, "Capacity enhancement using an interference limited area for device-to-device uplink underlying cellular networks," *IEEE Trans. Wireless Commun.*, vol. 10, pp. 3995–4000, Dec. 2011.
- [8] C.-H. Yu, O. Tirkkonen, K. Doppler, and C. Ribeiro, "On the performance of device-to-device underlay communication with simple power control," in *Proc. IEEE VTC-Spring*, Barcelona, Spain, Apr. 2009, pp. 1–5.
- [9] P. Jänis, C.-H. Yu, K. Doppler, C. Ribeiro, C. Wijting, K. Hugl, O. Tirkkonen, and V. Koivunen, "Device-to-device communication underlying cellular communications systems," *Int. J. Commun., Netw., Syst. Sci.*, vol. 2, pp. 169–178, June 2009.
- [10] K. Doppler, C.-H. Yu, C. Ribeiro, and P. Jänis, "Mode selection for device-to-device communication underlying an LTE-Advanced network," in *Proc. IEEE WCNC*, Sydney, Australia, Apr. 2010, pp. 1–6.
- [11] H. S. Chae, J. Gu, B.-G. Choi, and M. Chung, "Radio resource allocation scheme for device-to-device communication in cellular networks using fractional frequency reuse," in *Proc. IEEE APCC*, Kuala Lumpur, Malaysia, Oct. 2011, pp. 58–62.
- [12] P. Bao, G. Yu, and R. Yin, "Novel frequency reusing scheme for interference mitigation in D2D uplink underlying networks," in *Proc. IEEE IWCNC*, Cagliari, Italy, July 2013, pp. 491–496.
- [13] P. Jänis, V. Koivunen, C. Ribeiro, J. Korhonen, K. Doppler, and K. Hugl, "Interference-aware resource allocation for device-to-device radio underlying cellular networks," in *Proc. IEEE VTC-Spring*, Barcelona, Spain, Apr. 2009, pp. 1–5.
- [14] B. Kaufman and B. Aazhang, "Cellular networks with an overlaid device to device network," in *Proc. IEEE Asilomar Conf. Signals, Syst. Comput.*, Pacific Grove, USA, Oct. 2008, pp. 1537–1541.
- [15] J. Wang, D. Zhu, C. Zhao, J. Li, and M. Lei, "Resource sharing of underlying device-to-device and uplink cellular communications," *IEEE Commun. Lett.*, vol. 17, pp. 1148–1151, June 2013.

- [16] C.-H. Yu, K. Doppler, C. Ribeiro, and O. Tirkkonen, "Resource sharing optimization for device-to-device communication underlying cellular networks," *IEEE Trans. Wireless Commun.*, vol. 10, pp. 2752–2763, Aug. 2011.
- [17] D. Feng, L. Lu, Y. Yuan-Wu, G. Y. Li, G. Feng, and S. Li, "Device-to-device communications underlying cellular networks," *IEEE Trans. Commun.*, vol. 61, pp. 3541–3551, Aug. 2013.
- [18] —, "Optimal resource allocation for device-to-device communications in fading channels," in *IEEE GLOBECOM*, Atlanta, USA, Dec. 2013, pp. 3673–3678.
- [19] L. Wang and H. Wu, "Fast pairing of device-to-device link underlay for spectrum sharing with cellular users," *IEEE Commun. Lett.*, vol. 18, pp. 1803–1806, Oct. 2014.
- [20] R. Zhang, X. Cheng, L. Yang, and B. Jiao, "Interference-aware graph based resource sharing for device-to-device communications underlying cellular networks," in *Proc. IEEE WCNC*, Shanghai, China, Apr. 2013, pp. 140–145.
- [21] G. Yu, L. Xu, D. Feng, R. Yin, G. Y. Li, and Y. Jiang, "Joint mode selection and resource allocation for device-to-device communications," *IEEE Trans. Commun.*, vol. 62, pp. 3814–3824, Nov. 2014.
- [22] R. Yin, G. Yu, H. Zhang, Z. Zhang, and G. Y. Li, "Pricing-based interference coordination for D2D communications in cellular networks," *IEEE Trans. Wireless Commun.*, vol. 14, pp. 1519–1532, Mar. 2015.
- [23] D. Wu, J. Wang, R. Q. Hu, Y. Cai, and L. Zhou, "Energy-efficient resource sharing for mobile device-to-device multimedia communications," *IEEE Trans. Veh. Technol.*, vol. 63, pp. 2093–2103, Jun 2014.
- [24] S. M. Kay, *Fundamentals of Statistical Signal Processing: Estimation Theory*. New Jersey, USA: Prentice-Hall PTR, 1993.
- [25] Z. Q. Luo and S. Zhang, "Dynamic spectrum management: complexity and duality," *IEEE J. Sel. Topics Signal Process.*, vol. 2, pp. 57–73, Feb. 2008.
- [26] H. Kuhn, "The Hungarian method for the assignment problem," *Nav. Res. Logist. Quart.*, vol. 2, pp. 83–97, Mar. 1955.



Ali Ramezani-Kebrya (S'13) received the B.Sc. degree from the University of Tehran, Tehran, Iran, and the M.A.Sc degree from Queen's University, Kingston, Canada, respectively. Then he joined the Wireless Computing Lab (WCL) of the Department of Electrical and Computer Engineering, the University of Toronto, Toronto, Canada, where he is currently a Ph.D. candidate. His research interests cover the broad area of Internet of Things, with special emphasis on D2D/M2M/V2V systems, optimization, learning algorithms, and resource allocation.

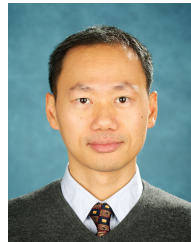
Mr. Ramezani-Kebrya was the recipient of the V. L. Henderson and M. Bassett Research Fellowship, the IEEE Kingston Section M.Sc. Research Excellence Award, and Ontario Graduate Scholarship (OGS).



Min Dong (S'00-M'05-SM'09) received the B.Eng. degree from Tsinghua University, Beijing, China, in 1998, and the Ph.D. degree in electrical and computer engineering with minor in applied mathematics from Cornell University, Ithaca, NY, in 2004. From 2004 to 2008, she was with Corporate Research and Development, Qualcomm Inc., San Diego, CA. In 2008, she joined the Department of Electrical, Computer and Software Engineering at University of Ontario Institute of Technology, Ontario, Canada, where she is currently an Associate Professor. She

also holds a status-only Associate Professor appointment with the Department of Electrical and Computer Engineering, University of Toronto since 2009. Her research interests are in the areas of statistical signal processing for communication networks, cooperative communications and networking techniques, and stochastic network optimization in dynamic networks and systems.

Dr. Dong received the the 2004 IEEE Signal Processing Society Best Paper Award, the Best Paper Award at IEEE ICC in 2012, and the Early Researcher Award from Ontario Ministry of Research and Innovation in 2012. She is the co-author of the Best Student Paper Award of Signal Processing for Communications and Networks in IEEE ICASSP'16. She served as an Associate Editor for the IEEE TRANSACTIONS ON SIGNAL PROCESSING (2010-2014), and as an Associate Editor for the IEEE SIGNAL PROCESSING LETTERS (2009-2013). She was a symposium lead co-chair of the Communications and Networks to Enable the Smart Grid Symposium at the IEEE International Conference on Smart Grid Communications (SmartGridComm) in 2014. She has been an elected member of IEEE Signal Processing Society Signal Processing for Communications and Networking (SP-COM) Technical Committee since 2013.



Ben Liang (S'94-M'01-SM'06) received honors-simultaneous B.Sc. (valedictorian) and M.Sc. degrees in Electrical Engineering from Polytechnic University in Brooklyn, New York, in 1997 and the Ph.D. degree in Electrical Engineering with a minor in Computer Science from Cornell University in Ithaca, New York, in 2001. In the 2001 - 2002 academic year, he was a visiting lecturer and post-doctoral research associate with Cornell University. He joined the Department of Electrical and Computer Engineering at the University of Toronto in 2002,

where he is now a Professor. His current research interests are in networked systems and mobile communications. He has served as an editor for the IEEE Transactions on Communications since 2014, and he was an editor for the IEEE Transactions on Wireless Communications from 2008 to 2013 and an associate editor for Wiley Security and Communication Networks from 2007 to 2016. He regularly serves on the organizational and technical committees of a number of conferences. He is a senior member of IEEE and a member of ACM and Tau Beta Pi.



Gary Boudreau (M'84-SM'11) received a B.A.Sc. in Electrical Engineering from the University of Ottawa in 1983, an M.A.Sc. in Electrical Engineering from Queens University in 1984 and a Ph.D. in electrical engineering from Carleton University in 1989.

From 1984 to 1989 he was employed as a communications systems engineer with Canadian Astronautics Limited and from 1990 to 1993 he worked as a satellite systems engineer for MPR Teltech Ltd. For the period spanning 1993 to 2009 he was employed

by Nortel Networks in a variety of wireless systems and management roles within the CDMA and LTE basestation product groups. In 2010 he joined Ericsson Canada where he is currently employed in the LTE systems architecture group. His interests include digital and wireless communications as well as digital signal processing.



Hossein Seyedmehdi received a Master's degree from the National University of Singapore in 2008 and a PhD degree from the University of Toronto in 2014 both in Electrical and Computer Engineering. He is currently affiliated with Ericsson Canada where he is working on the 5th generation (5G) of wireless technologies including the commercialization of massive MIMO. He has numerous papers in the area of wireless systems in addition to more than 10 patents. His research interests include Information Theory for Wireless Communications, Signal

Processing for MIMO channels, Algorithms for Radio Access Networks, and Future Radio Technologies.